Synaptic Relationships Between Dopaminergic Afferents and Cortical or Thalamic Input in the Sensorimotor Territory of the Striatum in Monkey

Y. SMITH, B.D. BENNETT, J.P. BOLAM, A. PARENT, AND A.F. SADIKOT
Centre de Recherche en Neurobiologie, Hôpital de l'Enfant-Jésus and Département d'Anatomie, Faculté de Médecine, Université Laval, Québec, Canada (Y.S., A.P., A.F.S.) and MRC Anatomical Neuropharmacology Unit, Oxford, United Kingdom (B.D.B., J.P.B.)

ABSTRACT

The cerebral cortex and the intralaminar thalamic nuclei are the major sources of excitatory glutamatergic afferents to the striatum, whereas the midbrain catecholaminergic neurones provide a dense intrastriatal plexus of dopamine-containing terminals. Evidence from various sources suggests that there is a functional interaction between the glutamate- and dopamine-containing terminals in the striatum. The aim of the present study was to determine the synaptic relationships between cortical or thalamic inputs and the dopaminergic afferents in the sensorimotor territory of the monkey striatum. To address this issue, anterograde tracing in combination with immunocytochemistry for tyrosine hydroxylase (TH) was carried out by light and electron microscopy.

Squirrel monkeys received injections of biocytin in the primary motor and somatosensory cortical areas or injections of either *Phaseolus vulgaris*-leucoagglutinin (PHA-L) or biocytin in the centromedian nucleus (CM) of the thalamus. Sections that included the striatum were processed to visualize the anterograde tracers alone or in combination with TH immunoreactivity. The anterogradely labelled fibres from the cerebral cortex and CM display a band-like pattern and are exclusively confined to the postcommissural region of the putamen, whereas TH-immunoreactive axon terminals are homogeneously distributed throughout the entire extent of the striatum. Electron microscopic analysis revealed that the anterogradely labelled terminals from the cerebral cortex form asymmetric synapses almost exclusively with the heads of dendritic spines. The thalamic terminals also form asymmetric synapses, but in contrast to cortical fibres, predominantly with dendrites (67.4%) and less frequently with spines (32.6%). The TH-immunoreactive boutons are heterogeneous in morphology. The most common type (84% of the total population) forms symmetric synapses; of these the majority is in contact with dendritic shafts (72.1%), less with spines (22.5%) and few with perikarya (5.4%). In sections processed to reveal anterogradely labelled cortical fibres and TH-immunoreactive structures, individual spines of striatal neurones were found to receive convergent synaptic inputs from both cortical and TH-immunoreactive boutons. In contrast, anterogradely labelled thalamic terminals and TH-immunoreactive boutons were never seen to form convergent synaptic contacts on the same postsynaptic structure.

These findings suggest that the dopaminergic afferents are located to subserve a more specific modulation of afferent cortical input than afferent thalamic input in the sensorimotor territory of the striatum in primates.

Key words: nigrostriatal pathway, dopamine, electron microscopy, thalamus, cerebral cortex

The striatum has long been known as a major target for glutamatergic terminals that mainly arise from the cerebral cortex (Divac et al., 1977; McGeer et al., 1977; Reubi and Cuénod, 1979; Hassler et al., 1982; Young and Bradford, 1986). Moreover, it is well established that the midbrain catecholaminergic neurones provide a dense plexus of dopa-

Accepted December 1, 1993.

Dr. Abbas F. Sadikot's present address is Dept. of Neurology and Neurosurgery, Montreal Neurological Institute, 3801 University street, Montréal, Québec, Canada, H3A 2B4.

Address reprint requests to Dr. Yoland Smith, Centre de Recherche en Neurobiologie, Hôpital de l'Enfant-Jésus, 1401, 18ième Rue, Québec, Canada G1J 1Z4.

mine-containing terminals that arborize profusely throughout the entire extent of the striatum (see Björklund and Lindvall, 1984 for a review). Evidence from various sources suggests a close interaction between the glutamate- and dopamine-containing terminals at the striatal level (see Nieoullon and Kerkerian-LeGoff, 1992 for a review). However, the exact mechanism by which these two populations of terminals interact to control the activity of striatal neurones is still controversial (Freund et al., 1984; Nieoullon and Kerkerian-LeGoff, 1992). Several pharmacological studies suggest reciprocal presynaptic interactions between dopamine- and glutamate-containing terminals in the striatum. These interactions are thought to be mediated by D2 dopaminergic receptors located on glutamatergic terminals, and N-methyl-D-aspartate (NMDA) or non-NMDA glutamate receptors located on dopaminergic afferents (see Nieoullon and Kerkérian-Le Goff, 1992 for a review). In apparent contradiction with these pharmacological data, ultrastructural studies indicated that the vast majority of catecholaminergic terminals form synapses with spines and dendritic shafts in the rat striatum (Pickel et al., 1981; Freund et al., 1984). However, the spines that receive input from the catecholaminergic afferents are often contacted more distally by boutons that display the morphological features of excitatory terminals (Freund et al., 1984). This synaptic arrangement led Freund et al. (1984) to suggest that one of the main functions of dopamine released from nigrostriatal terminals is to control the firing rate of striatal neurones by modulating their excitatory input at the level of individual spines. Although the exact origin of the excitatory terminals identified by Freund et al. (1984) remains to be established, it is almost certain that some of them arise from the cerebral cortex, which is a major source of terminals forming asymmetric synapses in the striatum (see Smith and Bolam, 1990a for a review). In fact, anatomical studies employing anterograde degeneration combined to immunocytochemical techniques for the detection of catecholaminergic terminals revealed that the cortical terminals and the catecholaminergic boutons converge on single spines and dendritic shafts in the dorsal striatum of the rat (Bouyer et al., 1984).

In addition to the cerebral cortex, another source of excitatory terminals forming asymmetric synapses in the striatum is the thalamus (Purpura and Malliani, 1967; Kemp and Powell, 1971; Kitai et al., 1976; Sadikot et al., 1992b). Although the thalamostriatal pathway arises from various nuclei, the major source of this projection is the caudal intralaminar nuclear group, namely the centromedian (CM) and the parafascicular (PF) nuclei (see Parent, 1986, 1990 for reviews). A recent anatomical investigation revealed that the thalamostriatal pathway arising from the CM and the PF in monkey is much more massive than previously thought, and occupies different territories in the striatum; the CM projects massively to the sensorimotor sector of the caudate nucleus and putamen, whereas the PF innervates predominantly the limbic-associative striatal territory (Sadikot et al., 1992a,b). At the ultrastructural level, both CM and PF terminals were found to form asymmetric synapses predominantly with dendritic shafts and less frequently with spines (Kemp and Powell, 1971; Sadikot et al., 1992b). Thus, the thalamus must also be considered as a major afferent to the striatum whose excitatory effect on striatal neurones may be modulated by the dopamine released from nigrostriatal axons. In fact, electrophysiological data suggested that the thalamus, cerebral cortex and substantia nigra converge on single spiny neurones in rat and cat striatum (Kitai et al., 1976; Kocsis et al., 1977; Vandermaelen and Kitai, 1980). However, before being able to speculate on the mechanism by which the thalamic and nigral afferents might interact at the striatal level, it is essential to better understand the synaptic relationship between these two sets of terminals.

The major aim of the present study was to elucidate the synaptic interactions between the thalamic and the dopaminergic afferents at the single cell level in the monkey striatum. In order to determine whether the two major excitatory inputs to striatal neurones interact in the same way with the dopaminergic afferents, the synaptic relationship between cortical and dopaminergic terminals was also examined.

Abbreviations

ABC	avidin biotinylated peroxidase complex
BDHC	benzidine dihydrochloride
Bio	biocytin
BSA	bovine serum albumin
CM	centromedian nucleus
CS	central sulcus
Ctx	cerebral cortex
DAB	3,3′ diaminobenzidine tetrahydrochloride
Den	dendritic shaft
EPSPs	excitatory postsynaptic potentials
FR	fasciculus retroflexus
FS	sylvian fissure
GPe	globus pallidus, external segment
GPi	globus pallidus, internal segment
MPTP	1-methyl-4-phenyl-1,2,3,6-tetrahydropyridine
Ni-DAB	nickel-enhanced diaminobenzidine
PB	phosphate buffer
PBS	phosphate-buffered saline
Per	perikaryon
PF	parafascicular nucleus
PHA-L	*phaseolus vulgaris*-leucoagglutinin
PU	putamen
SN	substantia nigra
SP	spine
sPF	subparafascicular nucleus
STS	superior temporal sulcus
TH	tyrosine hydroxylase
Thal	thalamostriatal terminals

MATERIALS AND METHODS

Animals and preparation of tissue

Nine adult male squirrel monkeys (*Saimiri sciureus*) were used in the present study. They were anesthetized with a mixture of ketamine hydrochloride (Ketaset, 70 mg/kg, i.m.) and xylazine (10 mg/kg, i.m.) before being fixed in a stereotaxic frame. In five animals, a total volume of 0.5 to 1.0 μl of biocytin (Sigma Chemical Company, St. Louis, MO; 4% in Tris buffer 0.05 M, pH 7.6) was delivered unilaterally at five to ten different locations (0.1 μl of biocytin/site) in the primary motor and somatosensory cortices (Fig. 1A). In three monkeys, 0.2–0.5 μl of biocytin was injected unilaterally in CM (Fig. 1B), whereas in the last animal, *Phaseolus vulgaris* -leucoagglutinin (PHA-L; Vector Laboratories, Burlingame, CA; 2.5% solution in phosphate buffer 0.01 M, pH 8.0) was delivered unilaterally in CM. The biocytin was delivered by means of a 10 μl Hamilton microsyringe with a sealed-on micropipette tip having a diameter that ranged from 50 to 70 μm. The PHA-L was loaded in glass micropipettes with a tip diameter ranging from 20 to 40 μm. It was then injected iontophoretically at four different locations along the antero-

posterior extent of CM with a 7 μA positive current for 20 minutes by a 7 seconds On/7 seconds Off cycle (Gerfen and Sawchenko, 1984). The stereotaxic coordinates were chosen according to the atlas of Emmers and Akert (1963).

After the appropriate survival period (36–48 hours for biocytin, 10 days for PHA-L), the animals were deeply anesthetized with an overdose of pentobarbital and perfusion-fixed with 500–700 ml of cold Ringer solution followed by 1.5 litres of fixative containing a mixture of 2% paraformaldehyde and 1% glutaraldehyde in phosphate buffer (PB, 0.1 M, pH 7.4). This was followed by 1 litre of cold PB. After perfusion, the brains were cut in 10 mm thick blocks in the transverse plane and placed in cold phosphate-buffered saline (PBS, 0.01 M, pH 7.4) until sectioning. The blocks were cut into 60 μm thick transverse sections with a vibrating microtome, collected in cold PBS and treated for 20 minutes with sodium borohydride (1% in PBS). The sections were repeatedly washed in PBS and processed to reveal the anterograde tracers and tyrosine hydroxylase (TH) immunoreactivity according to protocols suitable for light or electron microscopy.

Simultaneous localization of biocytin and TH

Light microscopy. In the eight animals that received biocytin injections, a series of sections containing the injection sites and a series including the striatum were incubated for 12–16 hours at room temperature with a mixture of avidin-biotin-peroxidase complex (ABC; Vector Laboratories; 1:100 dilution) and mouse anti-TH antibody (INCSTAR, Stillwater, MN; 1:1,000 dilution) in PBS containing 0.3% Triton X-100 and 1% bovine serum albumin (BSA; Sigma). They were then washed in PBS and Tris buffer (0.05 M, pH 7.6) before being placed in a solution containing 3,3′ diaminobenzidine tetrahydrochloride (DAB, 0.025%; Sigma), 0.01 M Imidazole (Fisher Scientific, Nepean, Ont., Canada) and 0.006% hydrogen peroxide for 10–15 minutes. The reaction was stopped by repeated washes in PBS. The sections were then incubated for 90 minutes at room temperature with biotinylated horse anti-mouse IgG (Vector Laboratories; 1:200 dilution) in PBS containing 0.3% Triton X-100 and 1% normal horse serum. After three washes (10 minutes each) in PBS, the sections were reincubated for 90 minutes at room temperature in ABC (1:100 in PBS/0.3% Triton X-100/1% BSA). The peroxidase bound to the TH was then revealed by placing the sections in Tris buffer containing DAB (0.025%), amonium nickel sulfate (Fisher Scientific, 0.35%) and hydrogen peroxide (0.0006%) for 10 minutes (see Wouterlood et al., 1987 for more details). These sections were then mounted on chrome alum/gelatin-coated slides, dehydrated and a coverslip was applied with Permount. A series of adjacent sections was stained with cresyl violet to determine the exact location of the biocytin injection sites.

Electron microscopy. A series of sections that included the striatum was processed for the simultaneous visualization of biocytin and TH at the electron microscopic level. The sections were placed in a cryoprotectant solution (PB, 0.05 M, pH 7.4, containing 25% sucrose and 10% glycerol) for 20–30 minutes. After having sunk, they were frozen at −80°C for 20 minutes. They were then thawed and washed many times in PBS before being processed to localize biocytin and TH according to the protocol described above, except that Triton X-100 was not included in the solutions and the incubation in the ABC/mouse anti-TH mixture was carried out at 4°C for 48 hours. Although biocytin was localized with DAB in every section, TH was localized either with benzidine dihydrochloride (BDHC, Sigma) or DAB. The sections that were incubated with BDHC were washed three to five times in PB (0.01 M, pH 6.8) before being preincubated in a solution of BDHC that was prepared according to Levey et al. (1986). After a 10 minute preincubation, the reaction was initiated by adding hydrogen peroxide to a final concentration of 0.005% in fresh BDHC solution. The reaction was terminated after 5–7 minutes by extensive washing in PB (0.01 M, pH 6.8) before processing for electron microscopy. The sections that were incubated with DAB were processed in the same way as those prepared for light microscopy. A series of sections was processed to localize biocytin alone with DAB as chromogen.

As controls, a few sections were incubated in solutions from which the mouse anti-TH antibodies were omitted.

Simultaneous localization of PHA-L and TH

Light microscopy. A series of sections containing the PHA-L injection site and a series containing the striatum were first incubated for 48 hours at 4°C with a mixture of goat anti-PHA-L (Vector Laboratories; 1:2,000) and mouse anti-TH (INCSTAR; 1:1,000) in PBS including 0.3% Triton X-100 and 1% normal rabbit serum. They were then washed in PBS and incubated for 90 minutes at room temperature in the biotinylated rabbit anti-goat IgG (Vector Laboratories; 1:200) when PHA-L was revealed first or biotinylated horse anti-mouse IgG (Vector Laboratories, 1:200) when TH was localized first. The secondary antibodies were diluted in the same solution as the primary antibodies. After this reaction, the sections were washed in PBS and placed in ABC (same dilution as above) for an additional 90 minutes. After several washes in PBS and then in Tris buffer (0.05 M, pH 7.6), the sections were placed in DAB to reveal the first antigen (see above). The sections were then incubated with the secondary antibody and ABC to localize the second antigen with nickel enhanced-DAB (Ni-DAB; see above) as the chromogen. They were then mounted on chrome alum/gelatin-coated slides, dried at room temperature, dehydrated and a coverslip was applied with Permount.

Electron microscopy. A series of sections including the striatum was processed to localize PHA-L and TH for electron microscopy. The sections were placed in the cryoprotectant solution, frozen at −80°C and incubated with antibody solutions similar to those used for light microscopy except that Triton X-100 was omitted. In most of the sections, PHA-L was revealed first with DAB and TH second with BDHC. However, in a few sections, the order was reversed, i.e., TH was revealed first with DAB and then PHA-L was revealed with BDHC. As controls, a series of sections including the postcommissural region of the putamen was incubated in solutions from which the primary antibodies were omitted in turn and replaced by normal serum.

Some sections including the sensorimotor region of the putamen were incubated to reveal either PHA-L or TH alone with DAB as the chromogen.

Processing for electron microscopy

The sections were washed in PB (0.01 M, pH 6.8, for those containing the BDHC reaction product or 0.1 M, pH 7.4, for those containing the DAB deposit only) before being postfixed in osmium tetroxide (1% solution in the corre-

sponding PB) for 20 minutes. They were then washed in PB and dehydrated in a graded series of alcohol and propylene oxide. Uranyl acetate was added to the 70% ethanol (30 minutes) to improve the contrast in the electron microscope. The sections were then embedded in resin (Durcupan ACM, Fluka) on microscope slides, put in the oven and cured for 48 hours at 60°C. After a careful examination of these sections in the light microscope, regions of interest were drawn, sometimes photographed, cut out from the slides and glued on the top of resin blocks with cyanoacrylate glue. Serial ultrathin sections were then cut on a Reichert-Jung Ultracut E ultramicrotome and collected on Pioloform-coated single slots nickel grids. They were stained with lead citrate (Reynolds, 1963) and examined in a Phillips 410 or a Hitachi H-7100 electron microscope.

Analysis of the material

The cortical or thalamic injection sites were charted from coronal sections at magnifications between 2× and 10× with a drawing tube connected to a Nikon light microscope. The exact location of the cortical injection sites was determined with respect to the distribution of giant pyramidal Betz cells of area 4 that could be visualized on the adjacent cresyl violet-stained sections. The biocytin injection sites were charted from single sections and then reconstructed on the cortical surface with respect to sulcal patterns.

The ultrastructural features and postsynaptic targets of TH-immunoreactive terminals and the anterogradely labelled cortical or thalamic boutons were determined in the electron microscope by scanning ultrathin sections of regions in the postcommissural putamen enriched in the corresponding terminals. Every labelled terminal was examined on 2–6 serial sections, photographed and measured at the level where the synaptic specialization was the longest by either Ultimage (Graftek, France) or MacStereology software prepared for Macintosh computers. The synaptic relationships between the TH-immunoreactive boutons and the cortical or thalamic terminals were analysed at the electron microscopic level in sections containing a high density of DAB- and BDHC-labelled structures. Since the DAB and BDHC reaction products could not be differentiated at the light microscopic level in sections that were postfixed in osmium tetroxide, the striatal regions were selected for ultrathin sectioning from material prepared for light microscopic analysis. Briefly, sections of striatum that were processed to reveal TH immunoreactivity and the anterogradely transported tracers with Ni-DAB and DAB, respectively, were scanned in the light microscope to identify the presence of areas where the two fields of terminals overlapped. Once such an area was found (Fig. 6), the corresponding region on the adjacent section processed to reveal the two sets of terminals with DAB and BDHC was cut out from the slide, mounted on blocks of resin, cut into serial ultrathin sections and examined in the electron microscope. The number of regions examined from each experimental group is indicated in Table 1. In order to ensure that the sections contained both DAB- and BDHC-labelled elements, the most superficial sections of the blocks were selected for electron microscopic analysis. Once a striatal element was found to form synapses with either type of labelled terminal and be apposed by the other, it was followed in 4–6 serial sections in order to determine whether it received convergent synaptic input from both sets of terminals.

RESULTS

Location of cortical and thalamic injection sites

The biocytin injection sites in the cerebral cortex extended through all cortical layers, along much of the extent of the primary motor and somatosensory cortices (Fig. 1A). In both cortical areas, the injection sites were characterized by a central core containing many neurones that appeared to be completely filled with the tracer. Some of the biocytin-labelled cells displayed the morphological features of large pyramidal neurones and extended their apical dendrites towards the superficial layers.

In the thalamus, the biocytin and PHA-L injection sites were centered on CM. In Figure 1B, the precise limits of the biocytin injection site that gave rise to the heaviest anterograde labelling in the postcommissural region of the putamen are illustrated at rostral, middle and caudal levels of CM. In this case, the injection site involved the entire rostrocaudal and dorsoventral extent of CM. Mediolaterally, the injection site occupied the central part of the nucleus. Although the biocytin did not diffuse in PF, the underlying subparafascicular nucleus (sPF) and the overlying mediodorsal nucleus were slightly contaminated by this injection (Fig. 2C). In another case, the biocytin injection site was larger and diffused more extensively along the pipette track in the mediodorsal nucleus. In the third case, the biocytin injection was smaller and confined to the ventral third of CM along its entire rostrocaudal extent. The PF, sPF and mediodorsal nuclei as well as any other neighbouring thalamic nuclei were not contaminated by this injection. However, a slight contamination of the pretectal area occurred caudally. In the single case that received an injection of PHA-L, the location of the tracer was similar to that charted in Figure 1B except that the sPF was not contaminated. Both biocytin and PHA-L resulted in the same pattern of staining in the vicinity of the injection sites, i.e., a central core containing a rich plexus of processes with many darkly stained perikarya (Fig. 2C).

Anterograde labelling and TH immunostaining in the striatum

Cortical afferents

Light microscopic observations. In the three cases that received injections of biocytin in the primary motor and somatosensory areas of the cerebral cortex, the overall pattern of anterograde labelling in subcortical structures was in keeping with that described in previous studies (see Jones, 1986 for a review). Briefly, rich plexuses of anterogradely labelled fibres and terminals were found in various thalamic structures including the reticular, ventrolateral, ventroposterior, and centromedian nuclei. The dorsolateral part of the subthalamic nucleus, the magnocellular region of the red nucleus and the superior colliculus also contained dense fields of labelled varicosities. Large labelled axons were found to travel caudalwards through the internal capsule, the cerebral peduncle and the reticular formation. Occasionally, one or two retrogradely labelled cells were found in the ventrolateral nucleus of the thalamus.

In the striatum, the biocytin-labelled structures included long linear and thin fibres as well as small varicosities that arborized profusely in the postcommissural region of the ipsilateral putamen. Occasionally, a small region along the dorsolateral edge of the caudate nucleus was weakly labelled. Contralaterally, the anterograde labelling was less

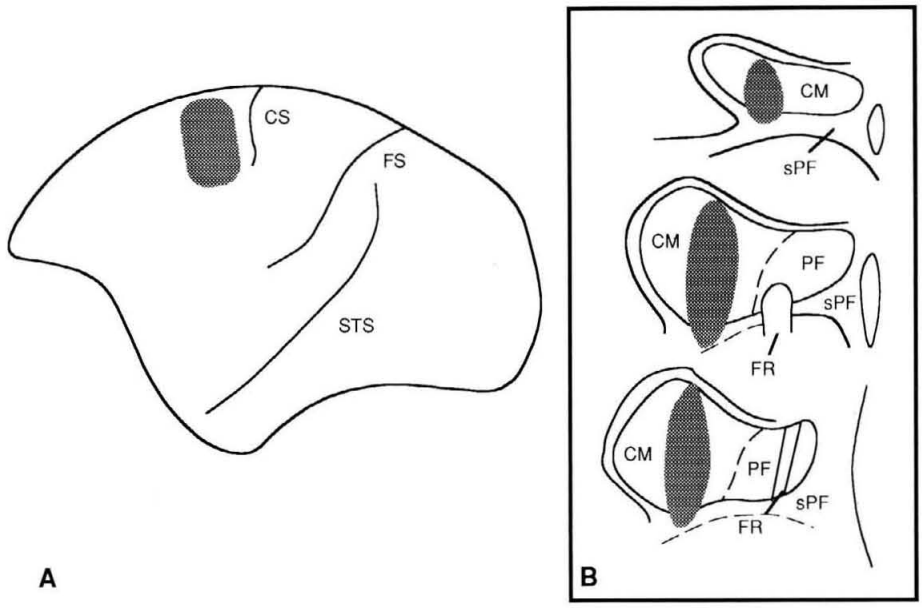

Fig. 1. **A:** Schematic drawing illustrating the location of the biocytin injection sites in the primary motor and somatosensory cortices of the squirrel monkeys. **B:** The boundaries of a biocytin injection site along the rostrocaudal (top to bottom) extent of CM. This thalamic injection gave rise to profuse anterograde labelling in the sensorimotor territory of the striatum. Note that the injection slightly contaminated the sPF but not the PF.

heavy but occurred in approximately the same striatal regions as was observed on the ipsilateral side. Although the anterograde labelling was heterogeneous throughout its entire rostrocaudal extent, it occurred in the form of patches rostrally (A14.0–12.0), but at more caudal levels (A12.0–6.5), the biocytin-labelled elements formed bands that occupied a large region of the ventrolateral two-thirds of the putamen. However, even in the most densely labelled region of the striatum, small areas were occasionally found to be completely devoid of anterograde labelling. Striatal regions rostral to A15.0 were devoid of staining.

Electron microscopic observations. The sections that were selected for analysis of labelled cortical terminals in the electron microscope were taken from regions containing the greatest density of stained terminals in the postcommissural putamen of three animals. In the electron microscope, the biocytin-labelled structures were easily differentiated from the unstained elements because of the electron-dense, amorphous, DAB reaction product associated with them (Fig. 2A,B). The biocytin-labelled fibres and varicosities observed in the light microscope were identified as nonmyelinated axons and vesicle-containing boutons, respectively. In the anterogradely labelled structures, the peroxidase reaction product was attached to the outer surface of electron-lucent vesicles, microtubules, and mitochondria, and to the inner surface of the plasmalemma (Fig. 2A,B). A total of 142 biocytin-labelled cortical boutons were photographed and analysed in random searches of electron microscopic sections. The morphological features, cross-sectional area and postsynaptic targets of these boutons were similar in the three animals. Although the size of these terminals was quite variable (mean cross-sectional area ± S.D. = 0.46 ± 0.22 μm^2; Fig. 4A), they all displayed the same morphological features, i.e., packed with round electron-lucent vesicles and a few mitochondria. In serial sections, all of the biocytin-labelled cortical boutons that were examined formed asymmetric synapses (Figs. 2A,B, 7). In 131 cases, the postsynaptic targets were dendritic spines characterized by the presence of a spine apparatus and the absence of mitochondria. In the remaining 11 cases, the exact nature of the postsynaptic targets could not be determined. In general, the heads of spines that received synaptic inputs from anterogradely labelled cortical terminals were large (0.5–1.5 μm in diameter) and contained a well-developed spine apparatus (Fig. 2A,B).

Thalamic afferents

Light microscopic observations. The biocytin and PHA-L injection sites in CM resulted in profuse anterograde labelling in various subcortical structures including the striatum. The pattern of distribution of the anterogradely labelled elements visualized in the present material was in keeping with that described recently by Sadikot et al. (1992a). The reader is referred to this study for a more detailed description of the subcortical efferent connections of CM in squirrel monkey (*Saimiri sciureus*). No retrogradely labelled neurones were found in the cerebral cortex after thalamic injections.

At the level of the striatum, a common characteristic of the four cases that received injections of anterograde tracer in CM was that the labelled thin fibres and small varicosities were found predominantly in the sensorimotor territory of the striatum. The precommissural regions of the caudate nucleus and putamen (A15.0–13.5) were almost completely devoid of labelled elements except for small patches of varicose fibres that were randomly dispersed in the dorsal half of the putamen and the dorsolateral part of the caudate nucleus close to the internal capsule. However, in the case that received a PHA-L injection that did not involve the sPF, the anterograde labelling rostral to the anterior commissure was much less abundant, whereas the postcommissural region of the putamen still contained rich plexuses of anterogradely labelled elements. In the four

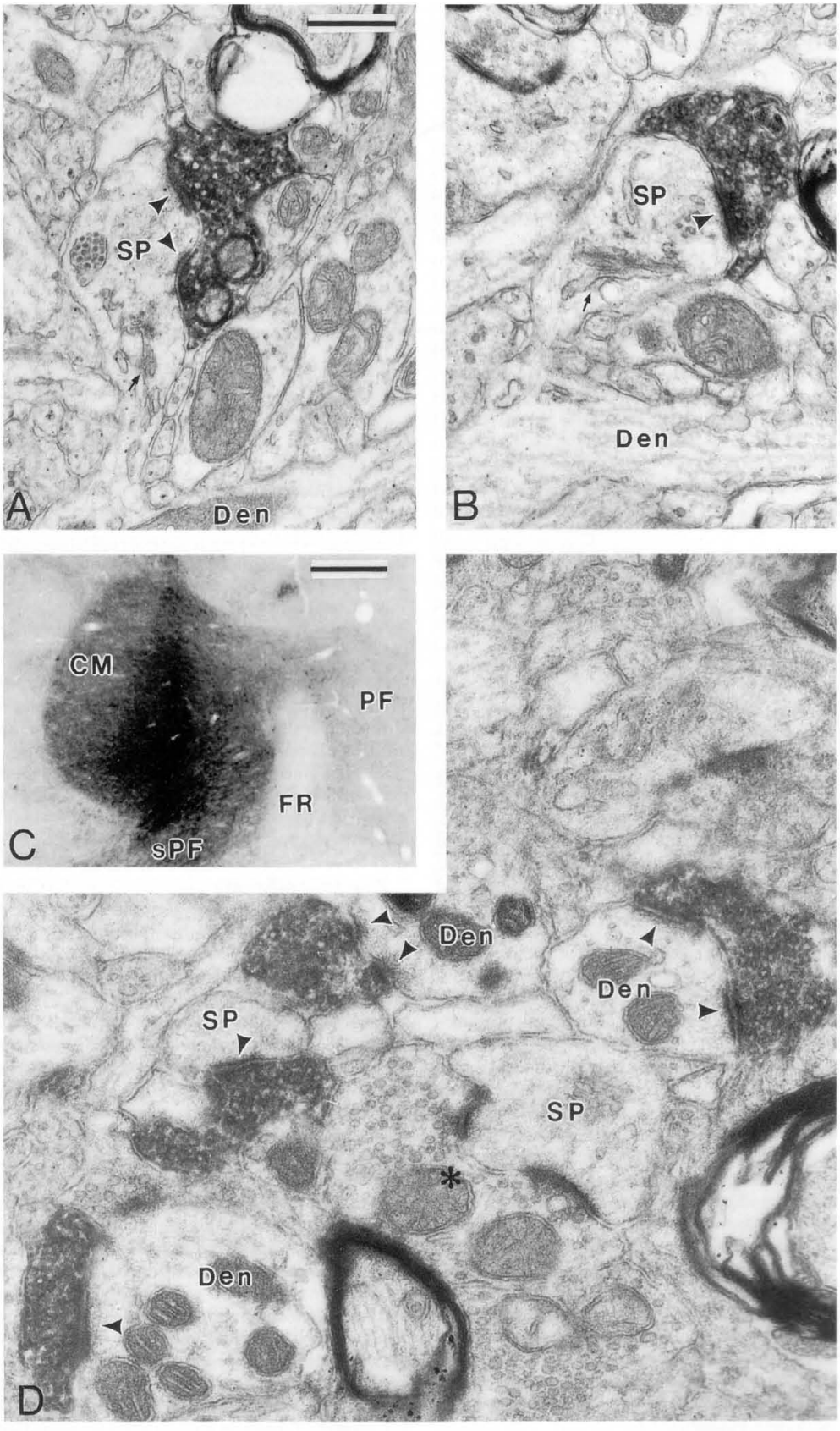

Figure 2

cases analysed in the present experiment, the striatum anterior to A15.0 was devoid of staining. As was the case for the cortical afferents, the anterogradely labelled fibres and terminals after CM injections displayed a band-like pattern in the postcommissural region of the putamen. Although the striatal territory occupied by the thalamic afferents was roughly similar to that innervated by the cortical input, the bands of thalamic labelling occurred throughout the full extent of the putamen in the mediolateral plane, whereas the cortical labelling was confined to the lateral two-thirds of the putamen. However, unlabelled regions between dense bands of anterograde labelling were always found in the putamen, and this occurred even in the areas of densest staining (A10.0–8.0).

Electron microscopic observations. At the electron microscopic level, the peroxidase reaction product was associated with axonal structures in the postcommissural region of the putamen after biocytin or PHA-L injection in CM. The anterogradely labelled elements included vesicle-containing boutons and myelinated or nonmyelinated axons. A total of 209 anterogradely labelled terminals were photographed and used for quantitative analysis. The thalamostriatal terminals were less heterogeneous in size (mean cross-sectional area ± S.D. = 0.28 ± 0.12 μm^2; Fig. 4B) and slightly smaller than the corticostriatal terminals. The morphological features and postsynaptic targets of the CM-striatal terminals analysed in the present study were in keeping with those described previously (Sadikot et al., 1992b). Briefly, the anterogradely labelled boutons contained round electron-lucent vesicles and formed asymmetric synapses predominantly with dendritic shafts (67.4%) and less frequently with spines (32.6%; Figs. 2D; 5).

TH immunostaining

Light microscopic observations. The overall pattern of distribution of the TH-immunoreactive structures in the present material was in keeping with that previously described in primate (Lavoie et al., 1989) and nonprimate species (Hökfelt et al., 1984). In the striatum, thin TH-immunoreactive axonal varicosities and long varicose fibres formed a dense homogeneous network that invaded the entire extent of the structure. Although both the dorsal and ventral striata received a dense TH-immunoreactive innervation, the nucleus accumbens and the olfactory tubercle were slightly more intensely labelled than the caudate nucleus and putamen. The perikarya and dendrites were nonimmunoreactive. At the light microscopic level, the TH-immunoreactive varicosities did not show any particular neuronal association with striatal elements.

Electron microscopic observations. At the electron microscopic level, the TH immunoreactivity was confined to vesicle-containing profiles and nonmyelinated axons. Examination of 22 vesicle-containing TH-immunoreactive profiles that did not form a clear synapse in the section under analysis revealed that they all formed synaptic contacts with spines or dendritic shafts in one or two adjacent sections (Figs. 3A–C; 7; 8). In three cases, the synaptic specialization was visualized in two sections but was not apparent in the four other serial sections of the same profile, suggesting that the synaptic contacts established by the TH-positive terminals in the monkey striatum have a short active zone. Three major populations of TH-immunoreactive terminals were identified. Examination of 243 TH-positive presynaptic profiles revealed that the most common type (84%; n = 204) belonged to a population of boutons that had a small cross-sectional area (mean ± S.D. = 0.14 ± 0.09 μm^2; Fig. 4C) and contained large, round, synaptic vesicles as well as one or two mitochondria (Fig. 7C). These boutons formed symmetric synapses predominantly with dendritic shafts (72.1%), less frequently with spines (22.5%) and rarely with perikarya (5.4%; Fig. 5). A second category of TH-positive presynaptic structures consisted of vesicle-containing profiles that appeared as varicose swellings arising from thin fibres which were filled with large round synaptic vesicles (Fig. 3A,B). These profiles accounted for 12% (n = 29) of the total population of TH-positive presynaptic structures in the monkey striatum. The most common postsynaptic targets of these structures were dendritic shafts (93%) but occasionally they formed synapses with spines (7%). In some cases, the intervaricose part of the vesicle-filled axons formed symmetric synapses with dendrites. The third category of TH-positive vesicle-containing boutons (3% of the total population; n = 8) were large terminals (maximum diameter larger than 1.0 μm) that were packed with pleomorphic electron-lucent vesicles and many mitochondria (Fig. 3D,E). These terminals were closely apposed to perikarya (66%) and dendritic shafts (34%), but clear synaptic specializations could not be identified. The perikarya apposed by these terminals were small to medium-sized and contained a large unindented nucleus surrounded by a thin rim of cytoplasm. In addition, two TH-positive boutons were small, contained round vesicles and formed asymmetric synapses with a dendritic shaft and a perikaryon (Fig. 3C). None of these TH-immunoreactive profiles formed synapses with axon initial segments nor other presynaptic elements.

Labelling of cortical afferents combined with TH immunostaining

Light microscopic observations. At the light microscopic level, the anterogradely labelled fibres and terminals from the cerebral cortex were distinguishable from the TH-positive structures by the colour of the peroxidase reaction product associated with them. Thus, the biocytin-labelled axons from the cerebral cortex were brown (DAB reaction product) whereas the TH-immunoreactive structures were blue (Ni-DAB reaction product; Fig. 6). The pattern of distribution and the morphological features of the cortical and TH-positive elements in this material were similar to those described above from the tissue processed for single staining. At the striatal level, both the DAB and Ni-DAB reaction products were associated with thin linear fibres and small axonal varicosities. Although the TH-immunoreactive elements invaded the entire extent of the

Fig. 2. **A,B:** Electron micrographs of terminals anterogradely labelled with biocytin from the motor and somatosensory cortices. Each terminal forms asymmetric synapses (arrowheads) with the head of dendritic spines (SP) in the sensorimotor territory of the putamen. The dendritic shaft (Den) from which the spine emerges can be seen. The spine apparatus is indicated by small arrows. **C:** Low power light micrograph showing a biocytin injection site in the central part of CM. Note that the injection slightly contaminated the underlying sPF but did not diffuse into the PF. **D:** Electron micrograph showing a region in the sensorimotor putamen containing four anterogradely labelled terminals after biocytin injection in CM. Three of these boutons form synapses with dendrites (Den) whereas the other contacts a dendritic spine (SP). In each case the synaptic specialization is asymmetric (arrowheads). An unlabelled bouton forming an asymmetric synapse with a dendritic spine is indicated by an asterisk. Scale bars = 0.5 μm in A, which also applies to B and D, 1 mm in C.

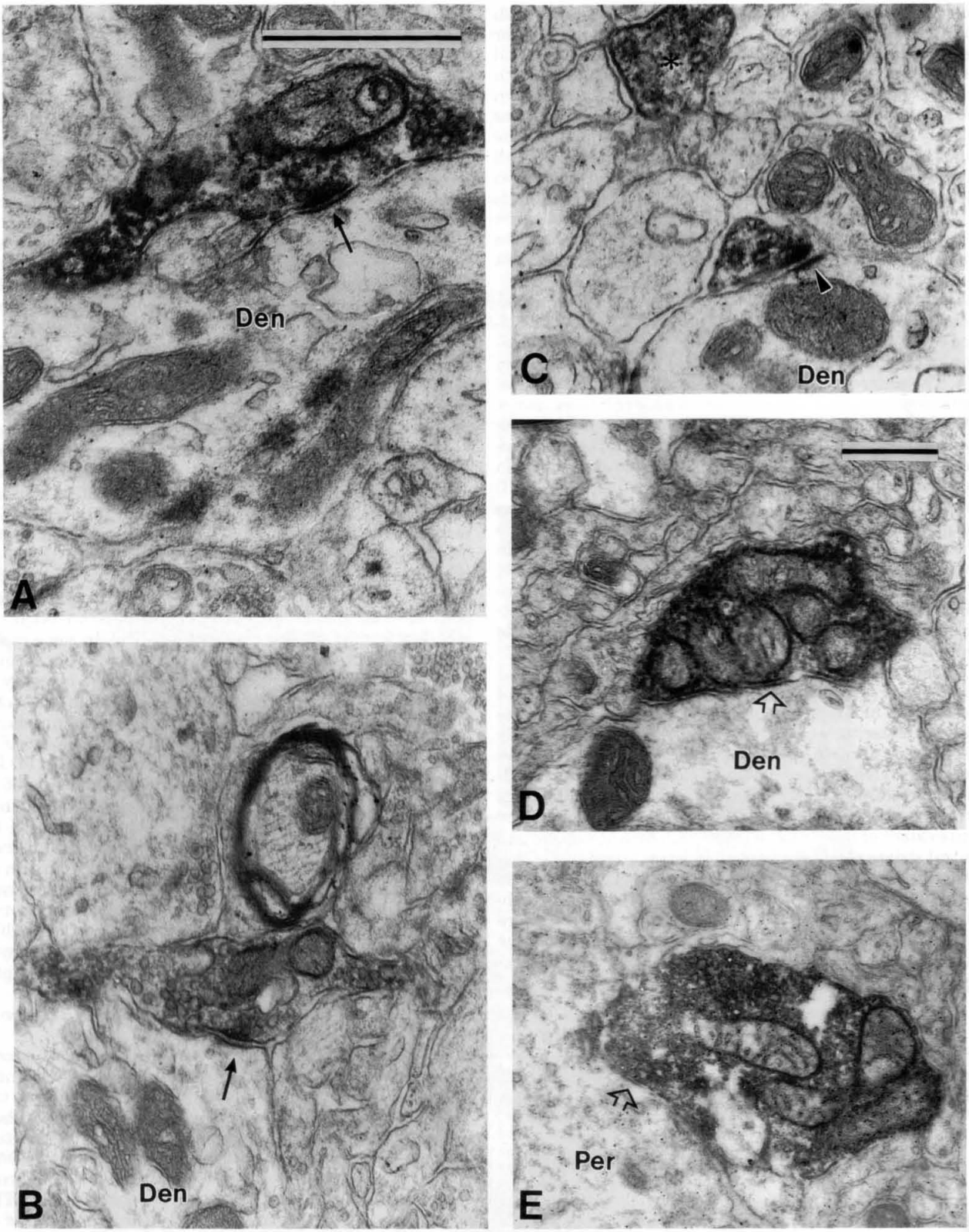

Fig. 3. Electron micrographs of TH-immunoreactive boutons in the sensorimotor territory of the monkey striatum. **A,B:** Two immunoreactive varicosities that arise from axons which are filled with electron-lucent vesicles. At the site of enlargement, the axon contains one or two mitochondria and forms "en passant" symmetric synapses (arrows) with dendritic shafts (Den). **C:** Small TH-immunoreactive bouton forming an asymmetric synapse (arrowhead) with a dendritic shaft (Den). Another TH-immunoreactive varicosity is indicated by an asterisk. **D,E:** Two large TH-positive terminals apposed to the surface of a dendritic shaft (Den; D) and a perikaryon (Per; E). Although these boutons are closely apposed to their targets (open arrowheads), clear synaptic specializations were not identified. Note that these terminals contain many more mitochondria than the other populations of TH-positive boutons. Scale bars = 0.5 μm in A, which also applies to B and C, 0.5 μm in D, which also applies to E.

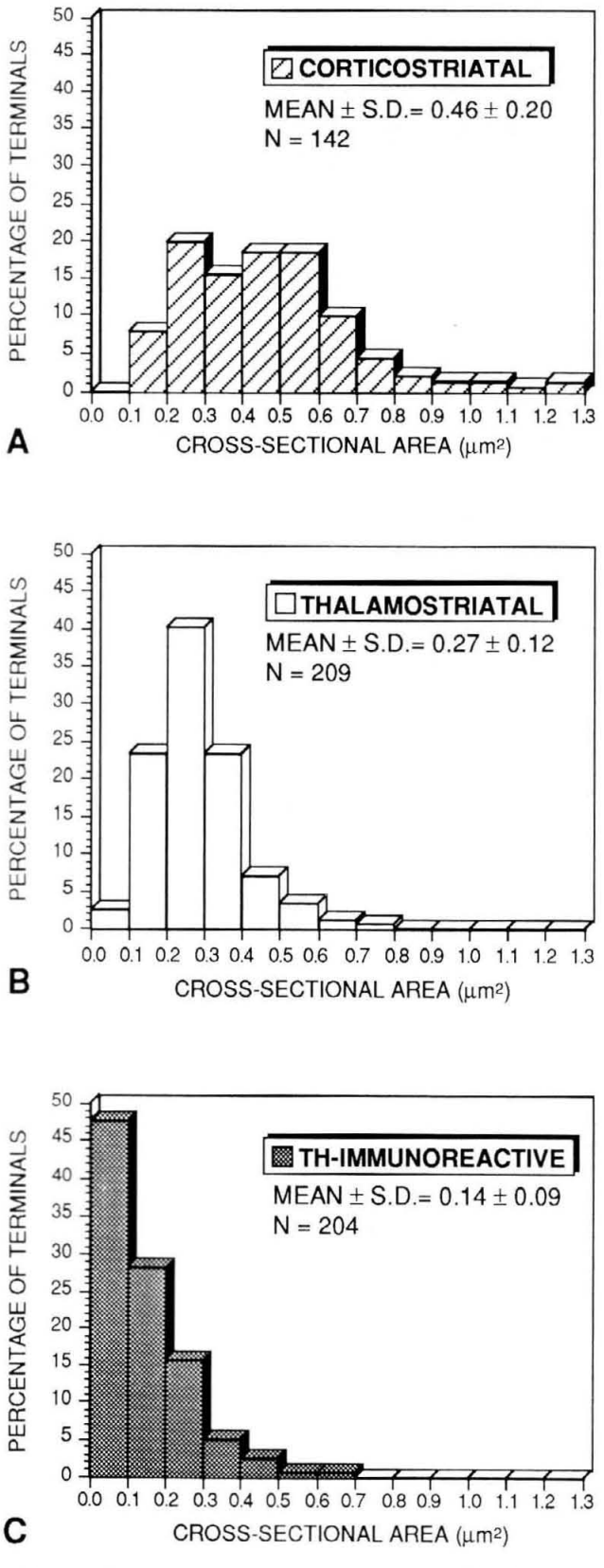

Fig. 4. Frequency distributions of the cross-sectional areas of corticostriatal (**A**), thalamostriatal (**B**) and TH-immunoreactive (**C**) boutons in the striatum of squirrel monkey. The TH-immunoreactive terminals included in these measurements belong to the most common population of TH-positive boutons (see Results).

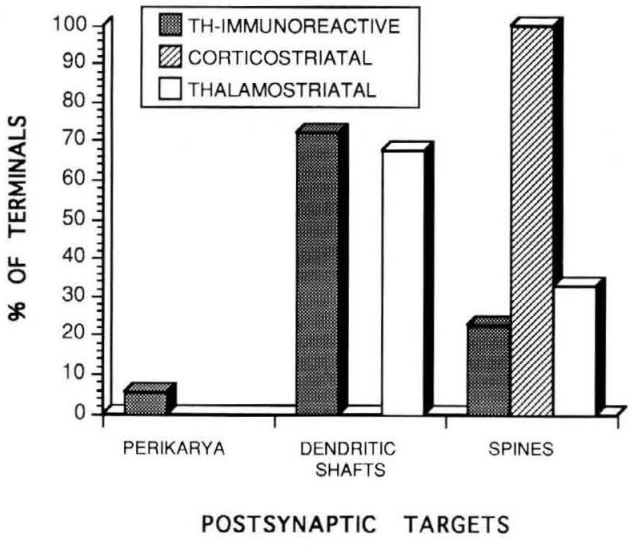

Fig. 5. Histogram comparing the relative distribution of the postsynaptic targets to corticostriatal, thalamostriatal and TH-immunoreactive boutons in the monkey striatum.

caudate nucleus and putamen, the anterogradely labelled fibres from the motor and somatosensory cortices were confined to the postcommissural region of the putamen. In this area, bands of anterogradely labelled axons and varicosities from the cerebral cortex overlapped with the TH-immunoreactive structures. However, even in the regions where the two fields were in register, it was still possible to distinguish the DAB- from the Ni-DAB-labelled elements (Fig. 6).

Electron microscopic observations. In the sections prepared for electron microscopy, the peroxidase reaction products associated with the cortical (DAB) and TH-immunoreactive (BDHC) structures were difficult to differentiate from each other at the light microscopic level. Therefore, the adjacent light microscopic sections processed with DAB and Ni-DAB were examined, and the areas of overlap served as a guide for the selection of appropriate regions for ultrathin sectioning in the material processed with DAB and BDHC. Using this approach, eight blocks were prepared, sectioned, and examined in the electron microscope for the presence of DAB-labelled cortical terminals and BDHC-labelled TH-positive structures. On the basis of previous experiments (Smith and Bolam, 1991; Bolam and Smith, 1992) indicating that the penetration of the BDHC reaction product is less than the DAB reaction product, the most superficial sections of the blocks were selected for ultrastructural analysis. At the electron microscopic level, the biocytin- and the TH-positive axon terminals were easily distinguishable by the texture of the peroxidase reaction product associated with them (Fig. 7). The DAB reaction product was amorphous, whereas the BDHC reaction product was in the form of electron-dense granules or crystals that were randomly dispersed throughout the labelled elements (Fig. 7).

In the eight blocks that were examined, both reaction products were present in the most superficial sections, and associated with presynaptic vesicle-containing profiles and myelinated or nonmyelinated axons. The morphological features of the cortical and TH-positive terminals were similar to those described above for single-stained material (Fig. 7). The synaptic interactions between the two popula-

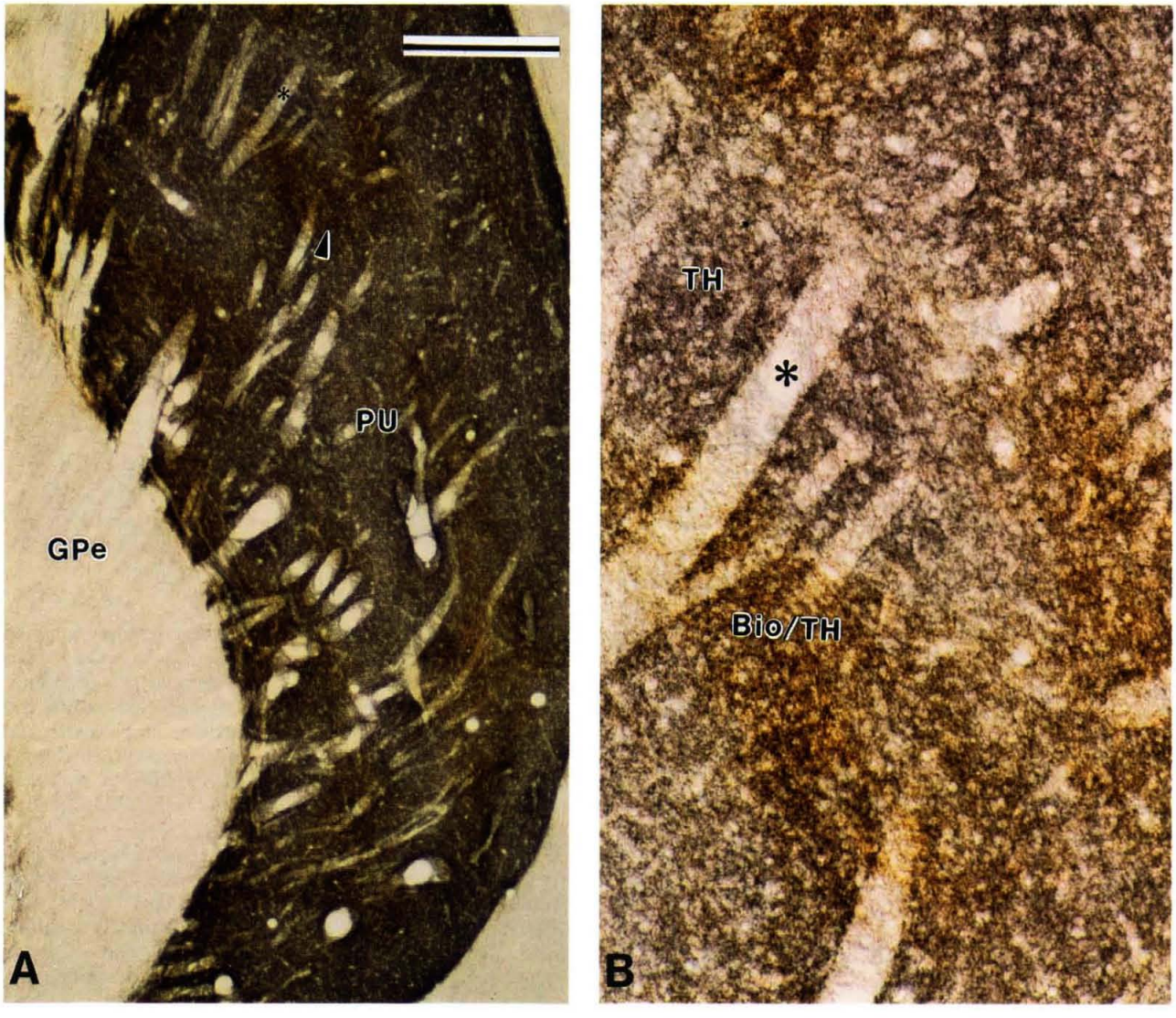

Fig. 6. Micrographs illustrating the close overlap between the fields of biocytin-labelled terminals from CM (DAB, brown) and TH-immunoreactive varicosities (Ni-DAB, blue) in the sensorimotor territory of the striatum (**A**). The zone of overlap indicated by an arrowhead is shown at higher magnification in (**B**). The asterisks indicate the same blood vessel in the two pictures. Scale bar = 1 mm for A; 0.25 mm for B.

tions of labelled terminals were analysed by examining serial sections of regions where the two populations of terminals were either apposed to single postsynaptic targets or in close proximity one another. In this way, forty-seven striatal elements were examined and five of them were found to receive convergent synaptic inputs from biocytin-labelled cortical terminals and TH-positive boutons (Fig. 7). In four cases, the two terminals converged on single spines (Fig. 7C,D) whereas in another case, the TH-immunoreactive bouton formed a synapse with the dendritic shaft and the cortical terminal established a synaptic contact with the head of the spine emerging from the same dendrite (Fig. 7A,B). In every case, the biocytin-labelled terminals formed asymmetric synapses, whereas the TH-positive boutons displayed the morphological features of the first category of TH-immunoreactive terminals described above and formed symmetric synaptic contacts (Fig. 7). The remaining striatal structures examined received an asymmetric synaptic contact from the biocytin-labelled terminals, but the synaptic specialization associated with the TH-positive boutons could not be identified with certainty. In none of the cases did the TH-immunoreactive boutons formed synapses with neighbouring structures. Direct synaptic contacts between the two populations of labelled terminals were not seen.

In the control sections that had been incubated in solutions from which the anti-TH antibodies were omitted, no BDHC-labelled axons or terminals were visualized. The only labelled structures contained the DAB reaction product and displayed the morphological features of cortical afferents.

Labelling of thalamic afferents combined with TH immunostaining

Light microscopic observations. At the light microscopic level, the TH-immunoreactive structures were distinguished from the anterogradely labelled fibres and varicosi-

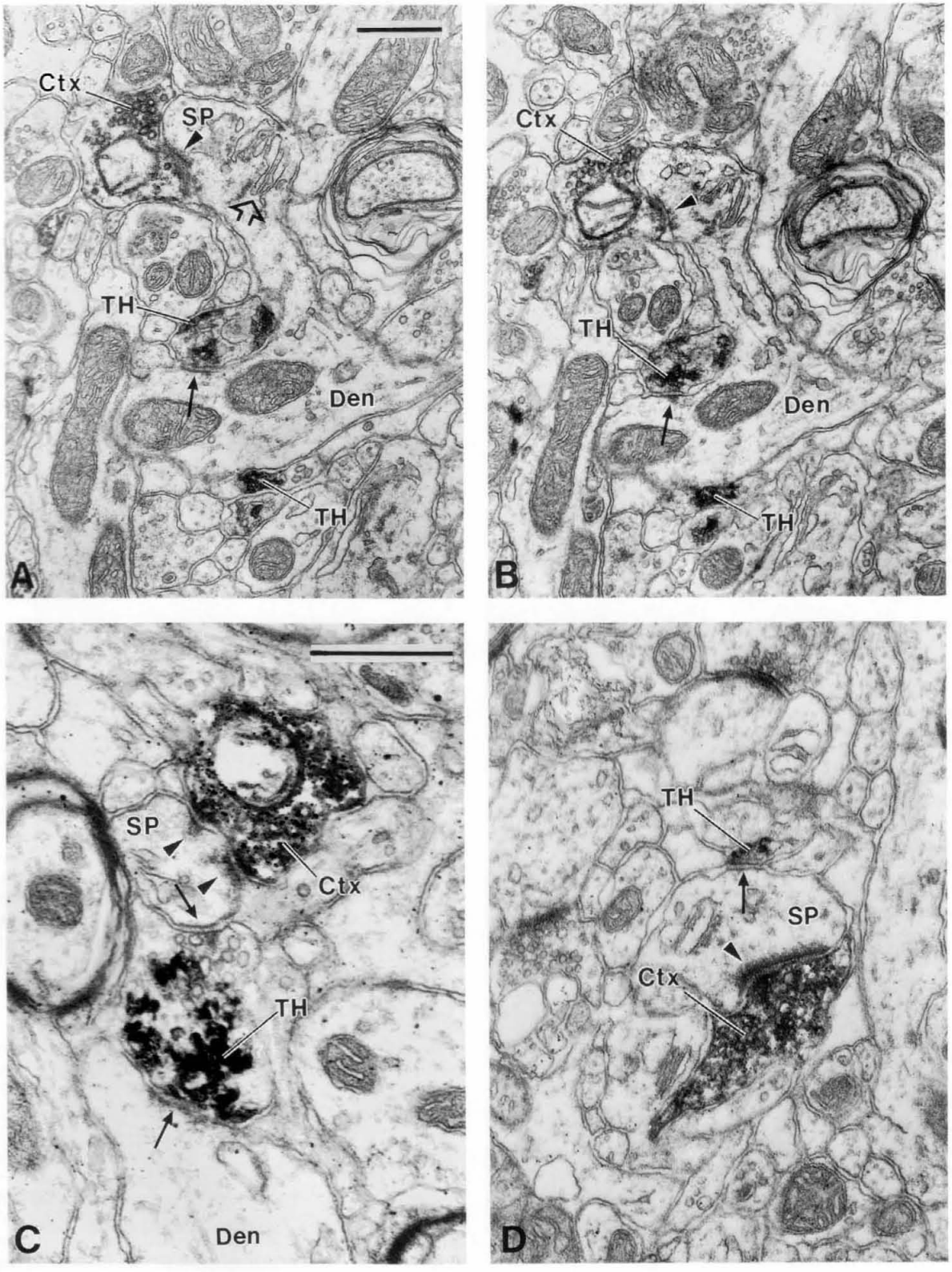

Fig. 7. Electron micrographs showing examples of striatal elements receiving convergent synaptic inputs from biocytin-labelled cortical terminals and TH-immunoreactive boutons. In this material, the TH-immunoreactive terminals were localized with BDHC and the biocytin-labelled boutons were localized with DAB. **A,B:** Serial sections of a dendritic shaft (Den) from which a spine (SP in A) emerges. The head of the spine forms an asymmetric synapse (arrowhead) with a biocytin-labelled cortical terminal (Ctx), whereas the dendritic shaft receives symmetric synaptic contact (arrow) from a TH-immunoreactive bouton. Another TH-positive terminal apposed to the surface of the dendrite is indicated. Note the prominent spine apparatus (open arrowhead in A). **C,D:** Heads of dendritic spines receiving both asymmetric synapses (arrowheads) from cortical terminals and symmetric synaptic contacts (arrows) from TH-positive boutons. In C, the TH-immunoreactive terminal is also in symmetric synaptic contact with a dendritic shaft. Scale bars = 0.5 μm in A, which also applies to B, 0.5 μm in C, which also applies to D.

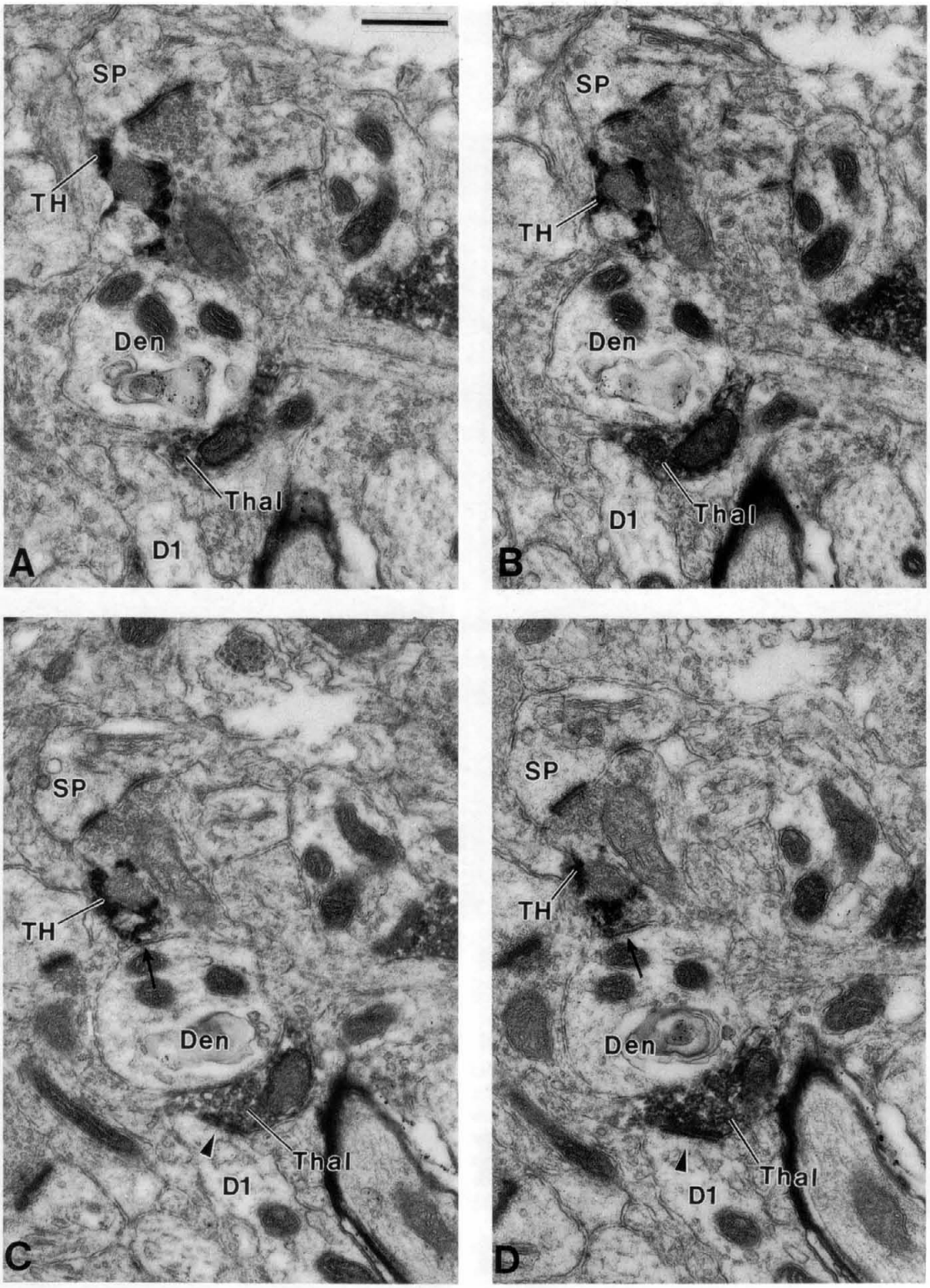

Fig. 8. **A–D:** Serial sections of a dendritic shaft (Den) apposed by a TH-immunoreactive terminal (BDHC-labelled) and a biocytin-containing (DAB-labelled) bouton anterogradely labelled from CM (Thal). **C,D:** The TH-positive terminal can be seen to form a symmetric synaptic contact with the dendrite (arrows). However, in the six serial sections examined (two are not illustrated), the biocytin-positive thalamic terminal did not establish a synaptic contact with the dendrite receiving input from the TH-positive bouton but formed an asymmetric synapse (arrowheads in C and D) with another dendtrite (D1) in the neuropile. A large head of a spine (SP) receiving an asymmetric synapse from an unlabelled bouton has been identified in the neuropile. Scale bar = 0.5 μm and applies to A–D.

TABLE 1. Summary of the Material Used and Results Obtained in the Double Labelling Experiments

Number of cases	Experimental protocol	Number of blocks	Number of sections examined	Number of appositions	Number of convergent synapses
5	Bio in Ctx/TH immuno.	8	25	47	5
3	Bio in CM/TH immuno.	27	135	6	0
1	PHA-L in CM/TH immuno.	6	30	0	0

ties by the colour of the reaction product associated with them (Fig. 6). The TH-immunoreactive elements were localized with Ni-DAB, whereas the anterogradely labelled fibres from the thalamus were labelled with DAB. As was the case after cortical injection, the fields of thalamic (DAB-labelled, brown) and TH-immunoreactive (Ni-DAB-labelled, blue) terminals closely overlapped in the postcommissural region of the putamen (Fig. 6).

Electron microscopic observations. In the sections prepared for electron microscopy, three different combinations of chromogens were used to localize the thalamic and TH-positive terminals in the striatum. In most of the sections, DAB was used to localize the anterogradely labelled thalamostriatal fibres, whereas BDHC served as the marker for TH-positive structures. In a few sections from the animal that received an injection of PHA-L in CM, the order was reversed, i.e., DAB was used to localize the TH-positive elements, whereas BDHC served as marker for the thalamostriatal fibres. Finally, a few sections from the case that resulted in the densest anterograde labelling in the striatum (Figs. 1B, 2C) were processed to localize both the biocytin-labelled terminals and the TH-positive elements with DAB. In the three types of material, the anterogradely labelled fibres from CM and the TH-immunoreactive terminals were difficult to distinguish at the light microscopic level. Therefore, the approach used to determine the appropriate areas for ultrathin sectioning was similar to that described above for the cortical and TH-positive boutons. Twenty-four of the areas selected were from material in which the biocytin-labelled thalamic terminals were localized with DAB and the TH-immunoreactive boutons with BDHC (see Table 1). Three blocks were taken from material in which both the biocytin- and the TH-positive elements were labelled with DAB. Four additional blocks contained DAB-labelled PHA-L-immunoreactive thalamic terminals and BDHC-labelled TH-positive boutons. In the two remaining blocks, the order was reversed, i.e., PHA-L was localized with BDHC and TH with DAB. In all the cases, the texture of the DAB and BDHC reaction products were easily distinguishable (see above).

The material that gave rise to the best results was that in which the biocytin-labelled thalamic terminals were labelled with DAB and the TH-immunoreactive boutons labelled with BDHC (Figs. 8,9). In such material, the DAB reaction product was associated with terminals displaying the morphological features of thalamic boutons, whereas the BDHC-labelled structures were typical of TH-immunoreactive elements. The synaptic relationships between the two populations of terminals were studied in the most superficial sections of the blocks containing the two peroxidase reaction products in the same tissue space. The approach was similar to that described above for the cortical and TH-positive terminals. A noticeable difference between this material and that processed to localize the cortical and TH-immunoreactive terminals was the paucity of structures in the striatum that were apposed by both sets of terminals (Table 1). In all the sections that were examined, only six dendritic shafts received synaptic contact from one population of terminals and at the same time were apposed by the other population (Table 1). In serial sections of each of these cases, the terminal that was apposed to the dendrite was not found to form a synapse with the dendrite receiving input from the other population of terminals, but rather formed synapses with adjacent structures in the neuropile (Fig. 8). In another case, a dendrite that received an asymmetric synaptic input from a biocytin-labelled terminal also formed a synaptic contact with another bouton that seemed to contain the BDHC reaction product (Fig. 9). However, when examined in serial sections, it became clear that the BDHC reaction product was not associated with the bouton forming the synaptic contact but with another terminal in the neuropile (Fig. 9).

In the material in which the TH was localized with DAB and PHA-L with BDHC, the DAB-labelled structures displayed the morphological features of TH-immunoreactive terminals, whereas the elements labelled with BDHC were typical of thalamostriatal boutons. Examination of areas containing both sets of terminals revealed that the two populations of labelled boutons formed synaptic contacts with different structures. However, the density of BDHC-labelled boutons arising from CM was much lower in this material than in the tissue processed to localize the thalamostriatal terminals with DAB. For this reason, most of the observations were made from the latter material.

In the sections containing both the thalamic and TH-positive elements localized with DAB, the criterion to differentiate the two populations of terminals was the synaptic specialization. On the basis of the observations described above, it was assumed that most of the labelled boutons forming asymmetric synapses arose from CM, whereas the labelled terminals forming symmetric synapses displayed TH immunoreactivity. Despite the fact that the selected area contained numerous terminals that could be categorized as arising from CM or immunoreactive for TH, striatal elements receiving convergent synaptic input from both sets of terminals were not observed.

DISCUSSION

The results of this study demonstrate that the dopaminergic afferents and the cortical input from the sensorimotor cortex converge on common postsynaptic targets in the sensorimotor territory of the striatum in squirrel monkey. In contrast, the dopaminergic afferents and the thalamic input from CM were not seen to converge on single postsynaptic targets in the same striatal territory. These findings suggest that the dopaminergic input interacts differently with cortical and thalamic afferents to influence the neuronal activity in the sensorimotor territory of the striatum in primate.

Corticostriatal and thalamostriatal afferents

The results of the present study demonstrate that striatal afferents arising from the primary motor and somatosen-

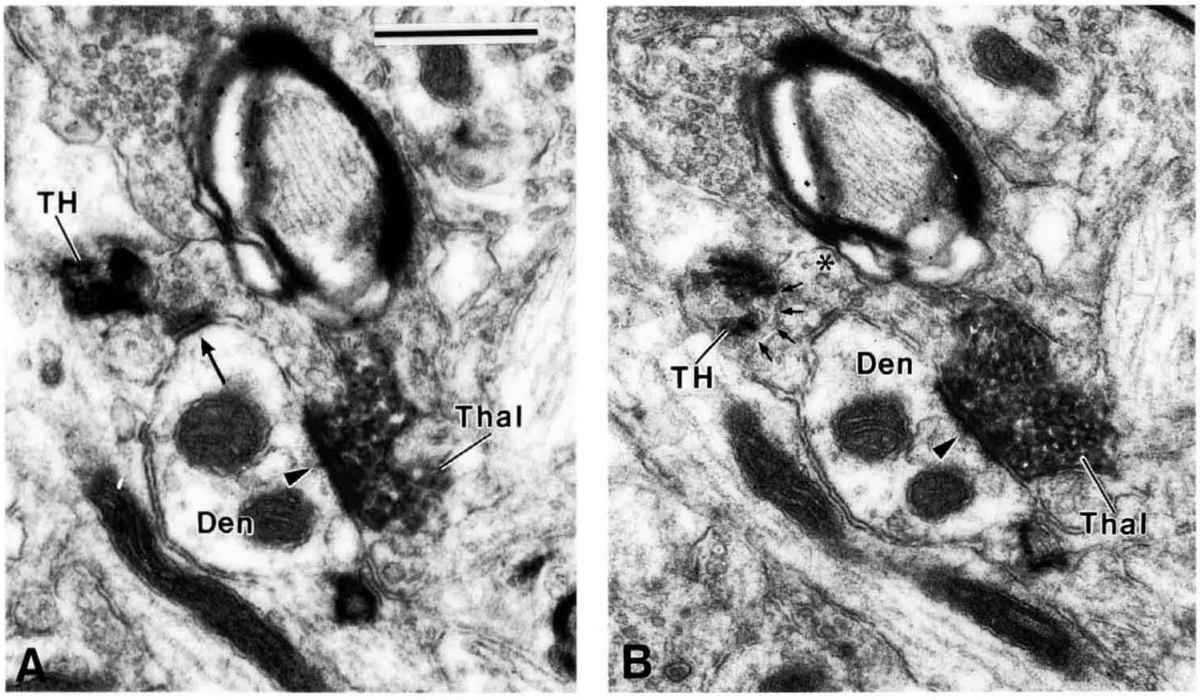

Fig. 9. **A,B:** Serial sections of a dendritic shaft (Den) receiving an asymmetric synapse (arrowheads) from a biocytin-containing bouton (DAB-labelled; Thal) anterogradely labelled from CM. The same dendrite receives symmetric synaptic contact (arrow) from another bouton, which in A seems to contain the BDHC reaction product indicating TH immunoreactivity. However, in B, it is clear that the BDHC reaction product is not associated with the bouton contacting the dendritic shaft (asterisk) but with another terminal in the neuropile. The small arrows indicate the membrane separating the two terminals. Scale bar = 0.5 μm and applies to A and B.

sory cortices in monkey terminate almost exclusively on the heads of dendritic spines. Previous ultrastructural data obtained in rat (Somogyi et al., 1981; Dubé et al., 1988; Wictorin et al., 1989; Xu et al., 1989; Lapper and Bolam, 1992), cat (Kemp and Powell, 1971; Hassler et al., 1978; Frotscher et al., 1981) and monkey (Lapper et al., 1992) are consistent with the fact that the major postsynaptic targets of cortical afferents in the striatum are dendritic spines. Furthermore, the ultrastructural features and synaptic specializations of the anterogradely labelled cortical terminals observed in the present study are in keeping with those described in other species by means of anterograde labelling or anterograde degeneration methods (Kemp and Powell, 1971; Somogyi et al., 1981; Bouyer et al., 1984; Wictorin et al., 1989; Lapper and Bolam, 1992). Although the major targets of the cortical afferents observed in the present study were dendritic spines, the possibility that dendritic shafts receive inputs from the primary motor and somatosensory cortices is not ruled out since a small proportion (8%) of striatal elements that formed synapses with the cortical terminals could not be identified. It is therefore possible that some of these unidentifiable targets were segments of dendritic shafts. In fact, axodendritic synapses formed by cortical boutons were observed in previous studies (Kemp and Powell, 1971; Frotscher et al., 1981; Wictorin et al., 1989; Xu et al., 1989; Lapper et al., 1992). Although they represented a small proportion of the total population of synapses formed by cortical boutons in the striatum, the axodendritic synaptic contacts may still be of functional importance since some of them are likely to be a source of direct cortical input to the aspiny striatal interneurones. In fact, axodendritic synapses between cortical terminals and parvalbumin-immunoreactive (Lapper et al., 1992) interneurones have been reported in monkey. Since the spiny neurones are the major population of striatal output cells (see Smith and Bolam, 1990a for a review), it would be important to determine the projection site of the striatal neurones contacted by the sensorimotor cortical afferents to better understand the anatomical organization of the corticostriatofugal pathway. It is particularly important to obtain such information in primates as the striatal afferents to the internal pallidum (GPi), external pallidum (GPe) and substantia nigra (SN) arise from distinct subpopulations of projection neurones (Féger and Crossman, 1984; Parent et al., 1984, 1989; Giménez-Amaya and Graybiel, 1990; Selemon and Goldman-Rakic, 1990).

Although the thalamostriatal projection arises from various nuclei in the thalamus of the primate and nonprimate species, it is clear that the intralaminar nuclei are the major source of thalamic afferents to the striatum (see Parent, 1990; Sadikot et al., 1992a,b for reviews). In a recent study using PHA-L as an anterograde tracer, Sadikot et al. (1992a,b) demonstrated that CM projects massively to the sensorimotor region of the putamen, whereas PF innervates predominantly the limbic-associative territory of the monkey striatum (Sadikot et al., 1992a). The results of the present study are consistent with those obtained by Sadikot et al. (1992a) since biocytin or PHA-L injections in CM led to massive anterograde labelling that was almost exclusively confined to the postcommissural region of the putamen. The ultrastructural morphology and postsynaptic targets of the thalamostriatal terminals examined in the present study were in keeping with those described in a previous communication (Sadikot et al., 1992b).

TH-immunoreactive terminals in the striatum

At the striatal level, a dense network of TH-immunoreactive fibres and terminals was distributed throughout the entire extent of the caudate nucleus and putamen. Although a minor contingent of these TH-immunoreactive elements may contain noradrenaline and arise from the locus coeruleus (Moore and Card, 1984; Smith and Parent, 1986), evidence from various sources suggests that the majority of TH-immunoreactive fibres and terminals in the dorsal striatum use dopamine as a neurotransmitter and arise from the substantia nigra pars compacta (see Björklund and Lindvall, 1984; Parent, 1986, 1990; Gerfen et al., 1987 for reviews). To our knowledge, no significant adrenergic input to the striatum has been described. We shall assume, therefore, that the TH-immunoreactive fibres that were observed in the present study are mainly fibres belonging to the nigrostriatal dopaminergic system.

An issue that is still controversial concerns the possibility that some of the TH-immunoreactive vesicle-containing profiles in the striatum release transmitter without forming synaptic contacts. In the rat, the proportion of TH-positive boutons that were reported to establish nonjunctional relationships with striatal elements varies significantly between different studies (Pickel et al., 1981; Arluison et al., 1984; Freund et al., 1984, Triarhou et al., 1988; Zahm, 1992). A common feature of those studies that reported large proportions of nonsynaptic relationships is that the analysis of TH-immunoreactive terminals was carried out in single ultrathin sections (Arluison et al., 1984; Triarhou et al., 1988; Zahm, 1992). In contrast, in those studies in which TH-immunoreactive terminals were followed through serial sections, the majority of boutons were seen to form symmetric synapses with dendrites and dendritic spines (Pickel et al., 1981; Freund et al., 1984). Our data are consistent with the hypothesis that most of the TH-immunoreactive boutons form synaptic contacts in the striatum. Examination through a complete set of serial sections of twenty-two vesicle-filled TH-immunoreactive profiles revealed that all of them established synaptic contacts. In this analysis, the synaptic specialization could only be visualized in one or two of the sections. Therefore, our data in monkey and those previously obtained in rodents (Pickel et al., 1981; Freund et al., 1984) demonstrate that nonsynaptic relationships between TH-immunoreactive boutons and striatal elements can only be ascertained if the immunoreactive terminals have been examined in a complete set of serial sections in material that has a good ultrastructural preservation.

In the present study, the TH-immunoreactive vesicle-containing profiles were divided into three groups according to their ultrastructural features and synaptic specializations. Overall, the ultrastructural characteristics and postsynaptic targets of TH-immunoreactive boutons in the monkey striatum are in keeping with those previously described in rodents (Pickel et al., 1981; Arluison et al., 1984; Freund et al., 1984). The majority of TH-immunoreactive boutons in the rat and monkey striata were small terminals that formed symmetric synapses with dendrites and dendritic spines. One population of TH-immunoreactive terminals which were rarely found in the present study but which have not been consistently reported in rodents (but see Zahm, 1992), were the large terminals often apposed to perikarya. The interesting feature of these terminals is that large TH-immunoreactive boutons, frequently associated with perikarya of striatal neurones, were found to be selectively spared in adult rat striatum after neonatal lesion of the nigrostriatal pathway with 6-hydroxydopamine (Pickel et al., 1992b).

In keeping with previous data in other species, the major postsynaptic targets of the TH-immunoreactive terminals in the striatum of monkey were spines and dendritic shafts of medium-sized spiny neurones (see Smith and Bolam, 1990a for a review). Although these neurones were commonly seen as an homogeneous population of output cells innervating the substantia nigra and the two segments of the globus pallidus, it is now well established that the striatal innervation of the substantia nigra, GPi (or entopeduncular nucleus in nonprimates) and GPe (or globus pallidus in nonprimates) arises from three distinct subpopulations of striatal cells in cat (Beckstead and Cruz, 1986) and monkey (Féger and Crossman, 1984; Parent et al., 1984, 1989; Giménez-Amaya and Graybiel, 1990; Selemon and Goldman-Rakic, 1990). Recent in situ hybridization studies suggested that the dopaminergic nigrostriatal pathway exerts opposite effects on the striatopallidal and striatonigral neurones in the rat (see Gerfen, 1992 for a review). It is reasonable to suggest that the opposite effects of dopaminergic afferents on the two major subpopulations of striatofugal neurones may be reflected at the synaptic level. At present, the only detailed information regarding the dopaminergic innervation of a particular population of striatal output cells is that of striatonigral neurones in the rat (Freund et al., 1984) and pigeons (Karle et al., 1992). In all the other studies addressing this issue (Kubota et al., 1986a,b; Pickel et al., 1992a), only the proximal region of the output cells was labelled. Since the dopaminergic afferents predominantly innervate the distal parts of medium-sized spiny neurones (see Smith and Bolam, 1990a), it is essential to examine these distal regions of the neurones to better understand the synaptic mechanism by which the nigral afferents control the activity of striatal projection neurones.

Dual labelling of TH-immunoreactive terminals and cortical or thalamic afferents

The main objective of the experiment was to compare the synaptic relationship between the TH-immunoreactive terminals and the cortical or thalamic afferents at the single cell level in the monkey striatum. The method chosen to address this issue was to anterogradely label the cortical or thalamic afferents with PHA-L or biocytin and to combine this with immunocytochemistry for TH. The tissue was then processed to simultaneously reveal the anterograde tracers and TH immunoreactivity by means of double immunocytochemical methods suitable for light and electron microscopic observations. The technical limitations of this approach have been discussed in detail in previous studies (Bolam and Ingham, 1990; Smith and Bolam, 1990b, 1991, 1992; Bolam and Smith, 1992; von Krosigk et al., 1992).

One of the major finding of the present study is that axon terminals from the primary sensorimotor cortices and the TH-immunoreactive boutons formed synapses with common postsynaptic targets in the sensorimotor territory of the striatum in squirrel monkey. Although only five striatal elements were found to receive convergent synaptic inputs from both sets of terminals, it should be remembered that many more structures that formed a synaptic contact with the cortical terminals were apposed by the TH-positive

boutons. However, because of the short active zone between TH-immunoreactive terminals and their postsynaptic targets (see above), combined with the fact that the ultrastructure of BDHC-containing TH-immunoreactive terminals were often damaged, the synaptic specialization associated with many of the TH-positive boutons labelled with BDHC could not be determined with certainty. Since most of the TH-positive terminals were found to establish synaptic contacts in rat (Pickel et al., 1981; Freund et al., 1984) and monkey (see above) striatum, it is likely that the proportion of striatal elements receiving convergent synaptic inputs from cortical and dopaminergic terminals is much higher than that reported in the present study. These findings are consistent with those previously obtained in the the rat by means of anterograde degeneration method combined with TH immunocytochemistry (Bouyer et al., 1984). Moreover, electrophysiological data suggested that neurones in the dorsal striatum activated by cortical stimulation also respond to stimulation of the substantia nigra (Buchwald et al., 1973; Kitai et al., 1976; Kocsis et al., 1977; Vandermaelen and Kitai, 1980; Bishop et al., 1982), implying that there is convergence of cortical and nigral afferents onto single neurones in the rat and cat striatum. At the level of the ventral striatum, afferents from the hippocampus (Totterdell and Smith, 1989; Sesack and Pickel, 1990) or the prefrontal cortex (Sesack and Pickel, 1992) were found to converge with TH-immunoreactive neurones on common spiny neurones in the nucleus accumbens of the rat.

Electrophysiological data suggested that dopamine released from nigrostriatal terminals exerts a neuromodulatory action on the excitatory responses elicited by stimulation of the sensorimotor cortex in the rat (Hirata et al., 1984). Indeed, conditioning stimulation of the substantia nigra or iontophoretic application of dopamine was found to either enhance or attenuate the excitatory responses elicited by cortical stimulation (Hirata et al., 1984). Our ultrastructural data and those previously obtained in the rat (Bouyer et al., 1984; Freund et al., 1984) suggest that the modulatory effect of dopamine on the cortical afferents may be exerted at the level of individual spines in the striatum. In light of morphological studies, showing that the distal dendritic tree of the medium-sized spiny neurones are covered with spines, and that the head of spines often receive asymmetric synapses that mainly arise from the cerebral cortex (see Smith and Bolam, 1990a for a review), it is likely that single spiny neurones in the striatum are the targets of afferents arising from different cortical areas. If this is the case, then the major role of dopamine could be to facilitate the transmission of relevant cortical information and to suppress the unnecessary afferent information for the elaboration of a particular motor behaviour. This suggestion is supported by recent electrophysiological data showing that the somatosensory receptive fields of striatal neurones is larger in cats treated with 1-methyl-4-phenyl-1,2,3,6-tetrahydropyridine (MPTP) than in normal animals (Schneider, 1991). In MPTP-treated monkeys, the responses of pallidal neurones to passive limb movements were abnormally large, numerous and unselective (Miller and DeLong, 1987; Filion et al., 1988). However, the possibility that the sensory deficits of striatal neurones may be partly responsible for the abnormal responses of pallidal cells during passive limb movements remains to be established. Whatever the disruptions of the corticostriatopallidal system are in MPTP-treated animals, it is reasonable to believe that the sensorimotor deficits observed in Parkinson's disease are largely due to the loss of selective modulatory effect of dopamine upon specific cortical inputs to the spiny output neurones.

Although ultrastructural evidence suggests that dopaminergic and cortical terminals interact at a postsynaptic level to control the activity of single striatal neurones, various pharmacological studies suggest that this interaction occurs at the presynaptic level (see Nieoullon and Kerkérian-Le Goff, 1992 for a review) via D2 dopaminergic receptors located on cortical terminals. Our ultrastructural data and those previously obtained in the rat do not support such observations since axoaxonic synapses between TH-immunoreactive boutons and anterogradely labelled cortical terminals rarely occur in the striatum of both primate and nonprimate species (Bouyer et al., 1984; Freund et al., 1984; Totterdell and Smith, 1989; Sesack and Pickel, 1990, 1992). Although serial examination of TH-immunoreactive boutons in this and a previous study (Freund et al., 1984) suggests that most of these terminals form synaptic contacts, the possibility that nonsynaptic mechanisms underlie the modulatory interactions between cortical and dopaminergic terminals in the striatum is not ruled out. However, the presynaptic interactions between the dopaminergic and cortical afferents has been challenged by recent studies showing that D2 binding sites were almost completely lost following an axon-sparing lesion of the rat striatum, whereas cortical damage was ineffective at reducing the number of D2 receptors (Trugman et al., 1986; Joyce and Marshall, 1987).

In contrast to the cortical and TH-immunoreactive boutons which frequently converged on common postsynaptic targets, the thalamic terminals arising from CM and TH-immunoreactive boutons were not seen to form synapses on the same postsynaptic targets in the sensorimotor territory of the monkey striatum. It is unlikely that these negative findings are due to technical limitations since the same approach was used in both series of experiments (see above). Furthermore, about five times as much material from the thalamus experiment was examined in the electron microscope. These data do not rule out the possibility that the thalamic and TH-positive terminals form synapses on single striatal neurones, but if this is the case, then the two sets of terminals must innervate different parts of the neurones. This suggests that interactions between these two populations of terminals are much less specific than the interactions between cortical and TH-positive terminals. Intracellular recordings demonstrated that electrical stimulation of the CM/PF complex and the substantia nigra elicited convergent monosynaptic EPSPs in single spiny neurones in the rat and cat striatum (Kitai et al., 1976; Kocsis et al., 1977; Vandermaelen and Kitai, 1980). Although the modulatory effect of dopaminergic afferents on the corticostriatal projection is supported by anatomical, electrophysiological and pharmacological evidence (see above), such interaction between the thalamic and dopaminergic inputs to the dorsal striatum remains to be established. Nevertheless, microiontophoretic studies have demonstrated that the dopaminergic afferents from the ventral tegmental area exert a D1-mediated inhibitory effect on neurones in the nucleus accumbens receiving input from the parafascicular nucleus in the rat (Araike et al., 1984; Hara et al., 1989). Since the D1 receptors are predominantly located on postsynaptic sites in the striatum (Altar and Hauser, 1987; Huang et al., 1993; Levey et al., 1993; Yung et al., 1993), these findings suggest a functional

interaction between dopaminergic and thalamic afferents at the postsynaptic level in the nucleus accumbens. However, because the hodological and functional organization of the ventral striatum and dorsal striatum differ significantly (see Parent, 1986, 1990 for reviews), it is premature to suggest that a similar interaction occurs between dopaminergic afferents from the substantia nigra compacta and thalamic afferents from CM in the sensorimotor territory of the monkey striatum.

Concluding remarks

Our findings demonstrate that the terminals from sensorimotor cortical areas and the dopaminergic afferents from the substantia nigra frequently form synaptic contacts with common postsynaptic targets in the sensorimotor territory of the primate striatum. In contrast, the thalamic terminals from CM and the dopaminergic boutons innervate different postsynaptic targets in the same striatal territory. These ultrastructural data suggest that the nigrostriatal dopaminergic afferents interact differently with the two major excitatory inputs to the sensorimotor territory of the primate striatum. Although dopamine may exert a specific modulatory effect on afferent information arising from individual cortical terminals, the thalamostriatal input is not in a position to be as precisely controlled by the dopaminergic afferents. Since the role of the thalamostriatal pathway in the circuitry of the basal ganglia is still obscure, it is difficult to speculate on the functional significance of our findings. However, in light of recent anatomical data demonstrating that the thalamostriatal pathway arising from the posterior intralaminar nuclei is much more massive and better organized than previously thought (Sadikot et al., 1992a,b), combined with intracellular recordings suggesting that the thalamic afferents are as powerful as the cortical inputs in controlling the activity of neostriatal output neurones (Wilson et al., 1983), it is essential to determine the intrinsic striatal mechanism by which this afferent is modulated to better understand the role of this projection in the functional circuitry of the basal ganglia in primates.

ACKNOWLEDGMENTS

This work was supported by grants from the Medical Research Council (MRC) of Canada to Y. Smith (MT-1120) and A. Parent (MT-5781) and by the MRC of UK. The support from NATO (collaborative grant: CRG 890578) is acknowledged. Thanks are also due to Jean-François Paré, Isabelle Deaudelin, Frank Kennedy, Paul Jays, Caroline Francis, and Liz Norman for technical assistance. The authors acknowledge the Department of Pathology of the Enfant-Jésus hospital for the use of the Hitachi electron microscope. B.D. Bennett is supported by a studentship from the MRC of UK. A.F. Sadikot was supported by a fellowship from the Fonds de la Recherche en Santé du Québec.

LITERATURE CITED

Altar, C.A., and K. Hauser (1987) Topography of substantia nigra innervation by D1 receptor-containing striatal neurons. Brain Res. *410:*1–11.

Araike, A., M. Sasa, and S. Takaori (1984) Microiontophoretic studies of the dopaminergic inhibition from the ventral tegmental area to the nucleus accumbens neurons. J. Pharmacol. Exp. Ther. *229:*859–864.

Arluison, M., M. Dietl, and J. Thibault (1984) Ultrastructural morphology of dopaminergic nerve terminals and synapses in the striatum of the rat using tyrosine hydroxylase immunocytochemistry: A topographical study. Brain Res. Bull. *13:*269–285.

Beckstead, R.M., and C.J. Cruz (1986) Striatal axons to the globus pallidus, entopeduncular nucleus and substantia nigra come mainly from separate cell populations in cat. Neuroscience *19:*147–158.

Bishop, G.A., H.T. Chang, and S.T. Kitai (1982) Morphological and physiological properties of neostriatal neurons: An intracellular horseradish peroxidase study in the rat. Neuroscience *7:*179–191.

Björklund, A., and O. Lindvall (1984) Dopamine-containing systems in the CNS. In A. Björklund and T. Hökfelt (eds): Handbook of Chemical Neuroanatomy, Vol. II: Classical Neurotransmitters in the CNS, Part I. Amsterdam: Elsevier, pp. 55–122.

Bolam, J.P., and C.A. Ingham (1990) Combined morphological and histochemical techniques for the study of neuronal microcircuits. In A. Björklund, T. Hökfelt, F.G. Wouterlood, and A.N. van den Pol (eds): Handbook of Chemical Neuroanatomy, Analysis of Neuronal Microcircuits and Synaptic Interactions, Vol. 8. Amsterdam: Elsevier, pp. 125–198.

Bolam, J.P., and Y. Smith (1992) The striatum and the globus pallidus send convergent synaptic inputs onto single cells in the entopeduncular nucleus of the rat: A double anterograde labelling study combined with postembedding immunocytochemistry for GABA. J. Comp. Neurol. *321:*456–476.

Bouyer, J.J., D.H. Park, T.H. Joh, and V.M. Pickel (1984) Chemical and structural analysis of the relation between cortical inputs and tyrosine hydroxylase-containing terminals in rat neostriatum. Brain Res. *302:*267–275.

Buchwald, N.A., D.D. Price, L. Vernon, and C.D. Hull (1973) Caudate intracellular response to thalamic and cortical inputs. Exp. Neurol. *38:*311–323.

Divac, I., F. Fonnum, and J. Storm-Mathisen (1977) High affinity uptake of glutamate in terminals of corticostriatal axons. Nature *266:*377–378.

Dubé, L., A.D. Smith, and J.P. Bolam (1988) Identification of synaptic terminals of thalamic and cortical origin in contact with distinct medium-sized spiny neurons in the rat neostriatum. J. Comp. Neurol. *267:*455–471.

Emmers, R., and K. Akert (1963) A Stereotaxic Atlas of the Brain of the Squirrel Monkey (*Saimiri sciureus*). Madison: University of Wisconsin Press.

Féger, J., and A.R. Crossman (1984) Identification of different subpopulations of neostriatal neurones projecting to globus pallidus or substantia nigra in the monkey: A retrograde fluorescence double-labelling study. Neurosci. Lett. *49:*7–12.

Filion, M., L. Tremblay, and P.J. Bédard (1988) Abnormal influences of passive limb movement on the activity of globus pallidus neurons in parkinsonian monkeys. Brain Res. *444:*165–176.

Freund, T.F., J.F. Powell, and A.D. Smith (1984) Tyrosine hydroxylase-immunoreactive boutons in synaptic contact with identified striatonigral neurons, with particular reference to dendritic spines. Neuroscience *13:*1189–1215.

Frotscher, M., U. Rinne, R. Hassler, and A. Wagner (1981) Termination of cortical afferents on identified neurons in the caudate nucleus of the cat. A combined Golgi-EM degeneration study. Exp. Brain Res. *41:*329–337.

Gerfen, C.R. (1992) The neostriatal mosaic: Multiple levels of compartmental organization in the basal ganglia. Ann. Rev. Neurosci. *15:*285–320.

Gerfen C.R., and P.E. Sawchenko (1984) An anterograde neuroanatomical tracing method that shows the detailed morphology of neurons, their axons and terminals: Immunohistochemical localization of an axonally transported plant lectin, *Phaseolus vulgaris*-leucoagglutinin (PHA-L). Brain Res. *290:*219–238.

Gerfen, C.R., M. Herkenham, and J. Thibault (1987) The neostriatal mosaic: II. Patch- and matrix-directed mesostriatal dopaminergic and non-dopaminergic systems. J. Neurosci. *7:*3915–3934.

Giménez-Amaya, J.-M., and A.M. Graybiel (1990) Compartmental origins of the striatopallidal projection in the primate. Neuroscience *34:*111–126.

Hara, M., M. Sasa, and S. Takaori (1989) Ventral tegmental area-mediated inhibition of neurons of the nucleus accumbens receiving input from the parafascicular nucleus of the thalamus is mediated by dopamine D1 receptors. Neuropharmacology *28:*1203–1209.

Hassler, R., W.J. Chung, U. Rinne, and A. Wagner (1978) Selective degeneration of two out of the nine types of synapses in the cat caudate nucleus after cortical lesions. Exp. Brain Res. *31:*67–80.

Hassler, R., P. Haug, C. Nitsch, J.S. Kim, and K. Paik (1982) Effect of motor and premotor cortex ablation on concentration of amino acids, monoamines, and acetylcholine and on the ultrastructure in rat striatum. A

confirmation of glutamate as the specific cortico-striatal transmitter. J. Neurochem. *38:*1087–1098.

Hirata, K., C.Y. Yim, and G.J. Mogenson (1984) Excitatory input from sensory motor cortex to neostriatum and its modification by conditioning stimulation of the substantia nigra. Brain Res. *321:*1–8.

Hökfelt, T., R. Martensson, A. Björklund, S. Kleineau, and M. Goldstein (1984) Distribution maps of tyrosine hydroxylase-immunoreactive neurons in the rat brain. In A. Björklund and T. Hökfelt (eds): Handbook of Chemical Neuroanatomy, Vol. II: Classical Neurotransmitters in the CNS, Part I. Amsterdam: Elsevier, pp. 277–379.

Huang, Q., D. Zhou, K. Chase, J.F. Gusella, N. Aronin, and M. DiFiglia (1993) Immunohistochemical localization of the D1 dopamine receptor in rat brain reveals its axonal transport, pre- and postsynaptic localization, and prevalence in the basal ganglia, limbic system, and thalamic reticular nucleus. Proc. Natl. Acad. Sci. *89:*11988–11992.

Jones, E.G. (1986) Connectivity of the primate sensory-motor cortex. In E.G. Jones and A. Peters (eds): Cerebral Cortex, Vol. 5. New York: Plenum Press, pp. 113–183.

Joyce, J.N., and J.F. Marshall (1987) Quantitative autoradiography of dopamine D2 sites in rat caudate-putamen: Localization to intrinsic neurons and not to neocortical afferents. Neuroscience *20:*773–795.

Karle, E.J., K.D. Anderson, and A. Reiner (1992) Ultrastructural double-labeling demonstrates synaptic contacts between dopaminergic terminals and substance P-containing striatal neurons in pigeons. Brain Res. *572:*303–309.

Kemp, J.M., and T.P.S. Powell (1971) The termination of fibres from the cerebral cortex and thalamus upon dendritic spines in the caudate nucleus: A study with the Golgi method. Phil. Trans. R. Soc. Lond. (Biol) *262:*429–439.

Kitai, S.T., J.D. Kocsis, R.J. Preston, and M. Sugimori (1976) Monosynaptic inputs to caudate neurons identified by intracellular injection of horseradish peroxidase. Brain Res. *109:*601–606.

Kocsis, J.D., M. Sugimori, and S.T. Kitai (1977) Convergence of excitatory synaptic inputs to caudate spiny neurons. Brain Res. *124:*403–413.

Kubota, Y., S. Inagaki, and S. Kito (1986a) Innervation of substance P neurons by catecholaminergic terminals in the neostriatum. Brain Res. *375:*163–167.

Kubota, Y., S. Inagaki, S. Kito, H. Takagi, and A.D. Smith (1986b) Ultrastructural evidence of dopaminergic input to enkephalinergic neurons in rat neostriatum. Brain Res. *367:*374–378.

Lapper, S.R., and J.P. Bolam (1992) Input from the frontal cortex and the parafascicular nucleus to cholinergic interneurons in the dorsal striatum of the rat. Neuroscience *51:*533–545.

Lapper, S.R., Y. Smith, A.F. Sadikot, A. Parent, and J.P. Bolam (1992) Cortical input to parvalbumin-immunoreactive neurones in the putamen of the squirrel monkey. Brain Res. *580:*215–224.

Lavoie, B., Y. Smith, and A. Parent (1989) Dopaminergic innervation of the basal ganglia in the squirrel monkey as revealed by tyrosine hydroxylase immunohistochemistry. J. Comp. Neurol. *289:*36–52.

Levey, A.I., J.P. Bolam, D.B. Rye, A.E. Hallanger, R.M. Demuth, M.-M. Mesulam, and B.H. Wainer (1986) A light and electron microscopic procedure for sequential double antigen localization using diaminobenzidine and benzidine dihydrochloride. J. Histochem. Cytochem. *34:*1449–1457.

Levey, A.I., S.M. Herch, D.B. Rye, R. Sunahara, H.B. Niznik, C.A. Kitt, D.L. Price, R. Maggio, M.R. Brann, and B.J. Ciliax (1993) Localization of D1 and D2 dopamine receptors in rat, monkey, and human brain with subtype-specific antibodies. Proc. Natl. Acad. Sci. (in press).

McGeer, P.L., E.G. McGeer, U. Scherer, and K. Singh (1977) A glutamatergic corticostriatal path? Brain Res. *128:*369–373.

Moore, R.Y., and J.P. Card (1984) Noradrenaline-containing neuron systems. In A. Björklund and T. Hökfelt (eds): Handbook of Chemical Neuroanatomy, Vol. II: Classical Neurotransmitters in the CNS, Part I. Amsterdam: Elsevier, pp. 123–156.

Miller, W.C., and M.R. DeLong (1987) Altered tonic activity of neurons in the globus pallidus and subthalamic nucleus in the primate MPTP model of parkinsonism. In M.B. Carpenter and A. Jayaraman (eds): The Basal Ganglia II. New York: Plenum press, pp. 415–427.

Nieoullon, A., and L. Kerkérian-Le Goff (1992) Cellular interactions in the striatum involving neuronal systems using "classical" neurotransmitters: Possible functional implications. Mov. Disorders 7:311–325.

Parent, A. (1986) Comparative Neurobiology of the Basal Ganglia. New York: John Wiley & Sons.

Parent, A. (1990) Extrinsic connections of the basal ganglia. TINS *13:*254–258.

Parent, A., C. Bouchard, and Y. Smith (1984) The striatopallidal and striatonigral projections: Two distinct fiber systems in primate. Brain Res. *303:*385–390.

Parent, A., Y. Smith, M. Filion, and J. Dumas (1989) Distinct afferents to internal and external pallidal segments in the squirrel monkey. Neurosci. Lett. *96:*140–144.

Pickel, V.M., S.C. Beckley, T.H. Joh, and D.J. Reis (1981) Ultrastructural immunocytochemical localization of tyrosine hydroxylase in the neostriatum. Brain Res. *225:*373–385.

Pickel, V.M., J. Chan, and S.R. Sesack (1992a) Cellular basis for interactions between catecholaminergic afferents and neurons containing Leu-enkephalin-like immunoreactivity in rat caudate-putamen nuclei. J. Neurosci. Res. *31:*212–230.

Pickel, V.M., E. Johnson, M. Carson, and J. Chan (1992b) Ultrastructure of spared dopamine terminals in caudate-putamen nuclei of adult rats neonatally treated with intranigral 6-hydroxydopamine. Dev. Brain Res. *70:*75–87.

Purpura, D.P., and A. Malliani (1967) Intracellular studies of the corpus striatum. I. Synaptic potentials and discharge characteristics of caudate neurons activated by thalamic stimulation. Brain Res. *6:*324–340.

Reubi, J.C., and M. Cuénod (1979) Glutamate release in vitro from corticostriatal terminals. Brain Res. *176:*185–188.

Reynolds, E.S. (1963) The use of lead citrate at high pH as an electron opaque stain in electron microscopy. J. Cell. Biol. *17:*208–212.

Sadikot, A.F., A. Parent, and C. François (1992a) Efferent connections of the centromedian and parafascicular thalamic nuclei in the squirrel monkey: A PHA-L study of subcortical projections. J. Comp. Neurol. *315:*137–159.

Sadikot, A.F., A. Parent, Y. Smith, and J.P. Bolam (1992b) Efferent connections of the centromedian and parafascicular thalamic nuclei in the squirrel monkey: A light and electron microscopic study of the thalamostriatal projection in relation to striatal heterogeneity. J. Comp. Neurol. *320:*228–242.

Schneider, J.S. (1991) Responses of striatal neurons to peripheral sensory stimulation in symptomatic MPTP-exposed cats. Brain Res. *544:*297–302.

Selemon, L.D., and P.S. Goldman-Rakic (1990) Topographic intermingling of striatonigral and striatopallidal neurons in the rhesus monkey. J. Comp. Neurol. *297:*359–376.

Sesack, S.R., and V.M. Pickel (1990) In the rat medial nucleus accumbens, hippocampal and catecholaminergic terminals converge on spiny neurons and are in apposition to each other. Brain Res. *527:*266–279.

Sesack, S.R., and V.M. Pickel (1992) Prefrontal cortical efferents in the rat synapse on unlabeled neuronal targets of catecholamine terminals in the nucleus accumbens septi and on dopamine neurons in the ventral tegmental area. J. Comp. Neurol. *320:*145–160.

Smith, A.D., and J.P. Bolam (1990a) The neural network of the basal ganglia as revealed by the study of synaptic connections of identified neurones. TINS *13:*259–265.

Smith, Y., and J.P. Bolam (1990b) The output neurones and the dopaminergic neurones of the substantia nigra receive a GABA-containing input from the globus pallidus in the rat. J. Comp. Neurol. *296:*47–64.

Smith, Y., and J.P. Bolam (1991) Convergence of synaptic inputs from the striatum and the globus pallidus onto identified nigrocollicular cells in the rat: A double anterograde labelling study. Neuroscience *44:*45–73.

Smith, Y., and J.P. Bolam (1992) Combined approaches to experimental neuroanatomy: Combined tracing and immunocytochemical techniques for the study of neuronal microcircuits. In J.P. Bolam (ed): Experimental Neuroanatomy: A Practical Approach, Practical Approach Series #114. Oxford: Oxford University Press, pp. 239–266.

Smith, Y., and A. Parent (1986) Differential connections of the caudate nucleus and putamen in the squirrel monkey (*Saimiri sciureus*). Neuroscience *18:*347–371.

Somogyi, P., J.P. Bolam, and A.D. Smith (1981) Monosynaptic cortical input and local axon collaterals of identified striatonigral neurons. A light and electron microscopic study using the Golgi-peroxidase transport-degeneration procedure. J. Comp. Neurol. *195:*567–584.

Totterdell, S., and A.D. Smith (1989) Convergence of hippocampal and dopaminergic input onto identified neurons in the nucleus accumbens of the rat. J. Chem. Neuroanat. *2:*285–298.

Triarhou, L.C., J. Norton, and B. Ghetti (1988) Synaptic connectivity of tyrosine hydroxylase immunoreactive nerve terminals in the striatum of normal, heterozygous and homozygous weaver mutant mice. J. Neurocytol. *17:*221–232.

Trugman, J.M., W.A. Geary II, and G.F. Wooten (1986) Localization of D-2 dopamine receptors to intrinsic striatal neurones by quantitative autoradiography. Nature (Lond.) *323:*267–269.

Vandermaelen, C.P., and S.T. Kitai (1980) Intracellular analysis of synaptic potentials in rat neostriatum following stimulation of the cerebral cortex, thalamus, and substantia nigra. Brain Res. Bull. *5:*725–733.

von Krosigk, M., Y. Smith, J.P. Bolam, and A.D. Smith (1992) Synaptic organization of GABAergic inputs from the striatum and the globus pallidus onto neurons in the substantia nigra and retrorubral field which project to the medullary reticular formation. Neuroscience *50:*531–549.

Wictorin, K., D.J. Clarke, J.P. Bolam, and A. Björklund (1989) Host corticostriatal fibres establish synaptic connections with grafted striatal neurons in the ibotenic acid lesioned striatum. Eur. J. Neurosci. *1:*189–195.

Wilson, C.J., H.T. Chang, and S.T. Kitai (1983) Origins of post synaptic potentials evoked in spiny neostriatal projection neurons by thalamic stimulation in the rat. Exp. Brain Res. *51:*217–226.

Wouterlood, F.G., J.G.J.M. Bol, and H.W.M. Steinbusch (1987) Double-label immunocytochemistry: Combination of anterograde neuroanatomical tracing with *Phaseolus vulgaris*-leucoagglutinin and enzyme histochemistry of target neurons. J. Histochem. Cytochem. *35:*817–823.

Xu, Z.C., C.J. Wilson, and P.C. Emson (1989) Restoration of the corticostriatal projection in rat neostriatal grafts: Electron microscopic analysis. Neuroscience *29:*539–550.

Young, A.M.J., and H.F. Bradford (1986) Excitatory amino acid neurotransmitters in the corticostriate pathway: Studies using intracerebral microdialysis in vivo. J. Neurochem. *47:*1399–1404.

Yung, K.K.L., J.P. Bolam, A.D. Smith, S.M. Hersch, B.J. Ciliax, and A.I. Levey (1993) Ultrastructural localization of D1 and D2 dopamine receptors in the basal ganglia of the rat. Brain Res. Ass. Abstr. *10:*6.

Zahm, D.S. (1992) An electron microscopic morphometric comparison of tyrosine hydroxylase immunoreactive innervation of the neostriatum and the nucleus accumbens core and shell. Brain Res. *575:*341–346.